AWARD NUMBER: W81XWH-20-1-0908

TITLE: An Automatically Adjusting Dynamic Orthosis to Enhance Performance of Warfighters with Lower Limb Injury

PRINCIPAL INVESTIGATOR: Joan E Sanders PhD

CONTRACTING ORGANIZATION: University of Washington

REPORT DATE: October 2022

TYPE OF REPORT: Annual

PREPARED FOR: U.S. Army Medical Research and Development Command
Fort Detrick, Maryland 21702-5012

REPORT DOCUMENTATION PAGE

Form Approved
OMB No. 0704-0188

1. REPORT DATE	**2. REPORT TYPE**	**3. DATES COVERED**
Oct 2022	Annual	15 Sep 2021 – 14 Sep 2022

4. TITLE AND SUBTITLE

An Automatically Adjusting Dynamic Orthosis to Enhance Performance of Warfighters with Lower Limb Injury

5a. CONTRACT NUMBER
W81XWH-20-1-0908

5b. GRANT NUMBER

5c. PROGRAM ELEMENT NUMBER

6. AUTHOR(S)
Joan E Sanders PhD, Joseph L Garbini PhD

E-Mail: jsanders@uw.edu

5d. PROJECT NUMBER

5e. TASK NUMBER

5f. WORK UNIT NUMBER

7. PERFORMING ORGANIZATION NAME(S) AND ADDRESS(ES)

University of Washington
Seattle WA 98195

8. PERFORMING ORGANIZATION REPORT NUMBER

9. SPONSORING / MONITORING AGENCY NAME(S) AND ADDRESS(ES)

U.S. Army Medical Research and Development Command
Fort Detrick, Maryland 21702-5012

10. SPONSOR/MONITOR'S ACRONYM(S)

11. SPONSOR/MONITOR'S REPORT NUMBER(S)

12. DISTRIBUTION / AVAILABILITY STATEMENT

Approved for Public Release; Distribution Unlimited

13. SUPPLEMENTARY NOTES

14. ABSTRACT
In Year 2 the motor-driven adjustment system was modified to include two parts – one for adjustment of strut stiffness and the other for adjustment of DAFO angle (plantarflexion/ dorsiflexion adjustment). Much of our effort was focused on human participant testing to identify appropriate sensor metrics for the controller to maintain during running. DAFO deflection proved the most effective metric for strut stiffness adjustment, and peak bending moment timing expressed as a percentage of stance phase proved the most effective metric for DAFO angle adjustment. Modifications were made to the adjustable strut hardware to reduce its size and enhance the range of selectable stiffness settings. A range of 3 PDE levels was achieved. An effort to outsource production of the carbon fiber rear strut in the adjustable strut system was ineffective, though fabrication within our lab continues to be successful. The collected participant data strongly supports the hypothesis that the controller will make proper adjustments to account for disturbances, e.g., user running speed and' surface terrain.

15. SUBJECT TERMS
NONE LISTED

16. SECURITY CLASSIFICATION OF:			**17. LIMITATION OF ABSTRACT**	**18. NUMBER OF PAGES**	**19a. NAME OF RESPONSIBLE PERSON**
					USAMRDC
a. REPORT	**b. ABSTRACT**	**c. THIS PAGE**			**19b. TELEPHONE NUMBER** *(include area code)*
Unclassified	Unclassified	Unclassified	Unclassified	47	

Standard Form 298 (Rev. 8-98)
Prescribed by ANSI Std. Z39.18

TABLE OF CONTENTS

1. INTRODUCTION:

The rationale of this application is that Warfighters experience lower-limb injuries during combat that after surgical reconstruction may still limit their capability to return to duty. The objective is to create and test a technology to improve lower limb injured Warfighters' maximum running speed, running endurance, as well as maneuverability during non-running activities. The aims are to design an adjustable-stiffness dynamic brace to accomplish these objectives. Initially, the brace is adjusted using a mobile phone app while the person wearing the brace runs and walks. From the knowledge gained during those experiments, we design an automatically adjusting dynamic brace that has sensors, a small motor, and a small computer within it to make adjustment without distracting the user. Appropriate adjustment is made in real time according to what the user is doing. The automatically adjusting dynamic brace is tested both in the laboratory and in 4-week home studies, and its performance is compared with results from wearing a traditional dynamic brace.

2. KEYWORDS:

Dynamic AFO, auto-adjusting, limb reconstruction, lower-limb injury, orthosis, IDEO brace, return to duty, surgical reconstruction

3. ACCOMPLISHMENTS:

What were the major goals of the project?

The major goals of the project during Year 2 were to recruit and enroll able-bodied participants for Aim #2, to complete Aim #2 testing and analysis, and to have the automated system ready for out-of-lab testing. Targeted and actual completion dates for important phases of the project are listed below:

	Timeline	**Progress**	**Completion Date**
Major Task 1: Complete specifications and evaluate design	Months		
Hire personnel	1-3	100%	Nov 15 2020
Create support documents	1-3	100%	Dec 01 2020
Use CAD and FEM to generate candidates designs	4-6	100%	Apr 30 2021
Mechanically test candidates	4-6	100%	Sep 01 2021
Select single design for further development	6	100%	Sep 01 2021
Milestone Achieved: Single variable-stiffness strut design selected	6	100%	Sep 01 2021
Milestone Achieved: Prototype mechanism fabricated and tested	6	100%	Sep 14 2021
Major Task 2: Create electronics for DAQ and wireless control	Months		
Optimize componentry and circuit design, make board	7-9	100%	Aug 15 2021
Add mobile phone comm. and control of strut stiffness	7-9	100%	Jun 15 2021
Milestone Achieved: Electronics and wireless comm. done	9	100%	Aug 15 2021
Assemble, bench test, and modify if needed	10-12	100%	Sep 10 2021
Milestone Achieved: Unit ready for participant testing	12	100%	Sep 14 2021
Major Task 3: Prepare research protocol for controller develop.	Months		
Submit IRB and HRPO documents for Aim 2 approval	1-3	100%	Sep 14 2020
Milestone Achieved: IRB and HRPO approval for Aim 2 obtained	1-3	100%	Dec 18 2020
Major Task 4: Prepare research protocol for controller develop.	Months		
Recruit and enroll able-bodied participants	10-20	100%	Dec 31 2021 – Aug 04 2022
Milestone Achieved: 1st Aim 2 participant enrolled	13	100%	Dec 31 2021
Milestone Achieved: Aim 2 study begins	13	100%	Jan 12 2022
Complete able-bodied testing ($n \geq 3$)	13-22	100%	Oct 07 2022
Milestone Achieved: Able-bodied participant testing completed	22	100%	Oct 07 2022
Complete injury/reconstruction participant testing ($n \geq 3$)	16-28	10%	
Milestone Achieved: Limb injury/reconstr. partic. testing completed	28		
Complete data analysis	13-30		
Milestone Achieved: Automated control ready for out-of-lab testing	30		
Major Task 5: Prepare research protocol for crossover study	Months		
Submit IRB and HRPO documents for approval	1-3	100%	Sep 14 2020
Milestone Achieved: IRB and HRPO approval for Aim 3 obtained	1-3	100%	Dec 18 2020
Major Task 6: Conduct crossover study protocol	Months		
Recruit and enroll limb injury participants	28-40		

Milestone Achieved: 1st Aim 2 participant enrolled	
Milestone Achieved: Aim 3 study begins	
Complete testing first set of participants (*n=7*)	28-38
Milestone Achieved: Testing on first set of participants completed	36-38
Complete testing on second set of participants (*n=7*)	32-46
Milestone Achieved: Testing on second set of participants completed	44-46
Complete data analysis	46-48
Milestone Achieved: Manuscript submitted	48
Milestone Achieved: Final report submitted	48

What was accomplished under these goals?

Human Subject Testing Results

Eight participants have been recruited, 7 able-bodied and 1 person with ankle disability (Table 1). Six participants have been cast and research DAFOs fabricated for them. We included more than the original target number of 3 able-bodied participants because initial participants were similar in weight and stature, and we expected that a more physically diverse group would be more constructive towards the overall objectives of the project. Research DAFOs for the initial two pilot participants (P-1, P-2) tested in Year 1 were configured with the original sensor configuration described in the grant application – strain gages applied to the struts and footplate. The original double strut design was used – two parallel aluminum struts whose separation distance was controlled using a custom designed mechanism, accomplishing variable stiffness. Results from testing the two pilot participants were described in our Year 1 report. The first 3 full study participants (F1 to F3) used the modified double strut design which was an aluminum strut in parallel with a short carbon fiber strut. Separation distance was controlled using a more compact mechanism (Fig. 1a). Two inertial measurement units (IMUs), one on the cuff and one on the footplate, are now used to quantify cuff-footplate angle, which we termed DAFO deflection, during stance phase. We have also designed and tested a mechanism to plantarflex and dorsiflex the DAFO in anticipation of the need to control this variable to compensate for strut stiffness changes (Fig. 1b). At this point in the research, the two mechanisms are separate since including both would make the research DAFO too heavy. Once we have more experience using the mechanisms, we expect to be able to reduce their size. We have 2 alternate able-bodied participants (F-4, F-5) available should further able-bodied testing be required. One participant with ankle disability has been recruited and a research DAFO is being fabricated.

Table 1. Participants and Tests to Date

Recruited and Consented Participants	DAFO Sensors Used			Protocols – No. of Test Sessions/Completion Status			
	Strut SG	Ftplt SG	2 IMUs	Prelim.	Stiff-Gait	Aang-OuTerr	PlGain-TrTer
Pilot: able-bodied:							
P-1	X	X	-	14	-	-	-
P-2	X	X	-	11	-	-	-
Full: able-bodied:							
F-1	X	X	X	15	X	X	X
F-2	-	X	X	3	X	X	X
F-3	-	X	X	5	X	X	X
F-4 alt	-	X	X	1			
F-5 alt							
Full: lower-leg disability:							
D-1							

P= pilot study; F= full study; alt= alternate; No.= number; SG= strain gage; IMU= inertial measurement unit; Prelim.= preliminary; Stiff= stiffness; AAng= ankle angle; OuTerr= outdoor terrain; PlGain= plant gain; TrTerr= treadmill terrain; X= completed

Table 2. Full Study: Participant Characteristics

Participant	Gender	Age (y)	Height (cm)	Weight (kg)	Shoe Size	Disability
F-1	M	24	185	104	14.0W* men's	NA
F-2	M	25	178	84	11.0 men's	NA
F-3	F	54	172	62	8.5 women's	NA
F-4	F	61	163	61	8.5W women's	NA

F-5	F	48	152	54	7.0 women's	NA
D-1	M	61	188	92	12.0 men's	Ankle reconstruction

* W= wide

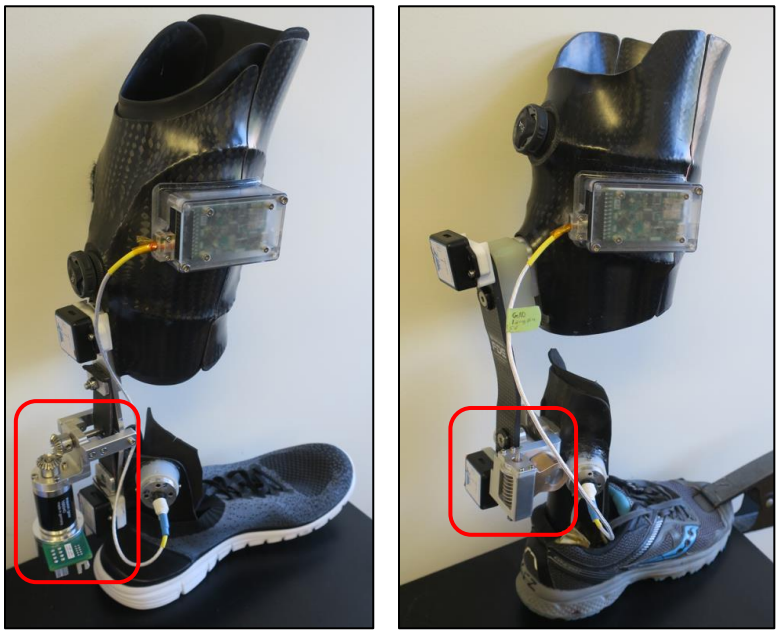

(a) (b)

Fig 1a.b. Adjustable DAFOs. (a) Mechanism to adjust strut stiffness. (b) Mechanism to adjust DAFO angle. The red boxes highlight the active parts of the mechanisms.

Preliminary tests on able-bodied full study participants

Relevant information was gained from 24 preliminary testing sessions conducted on participants F-1 to F-4. Results are summarized in Table 3.

Table 3. Principal Findings from Preliminary Testing on Able-Bodied Full Study Participants F-1 to F-4

Participant Session. finding	Result for Walk or Run?	Finding	Relevance	Figure
Participant F-1				
1 to 4.1	Walk	• Using the original design of the double-strut (as used by P-1 and P-2), instrumentation issues resolved	• The double-strut design works	-
5.1	Walk	• Using the new aluminum (Al)/carbon fiber double-strut design, instrumentation issues resolved	• The new double-strut design, smaller and lighter than the original design, works better	-
6.1	Walk	• Walking with an inactive ankle increased the intensity of the bending strain signal compared with an active ankle	• The active plantarflexion during late stance phase for the active ankle condition may counter the positive bending strain in the footplate • We may be able to quantify plantarflexion action using the footplate sensors	Fig. 2
6.2	Walk	• An uphill incline increased the intensity of the first peak in the bending strain signal	• Verification of sensor performance – result consistent with expectation	Fig. 2
6.3	Run	• Running immediately caused the Al strut in the new design to permanently deform	• Al strut needs to be re-designed to be more robust	-
7.1	Walk & Run	• Portable data acquisition unit used. Testing at different speeds and terrains (uphill, downhill) was successful. A PDE-5 strut was used instead of the double-strut	• System design is far along in terms of being ready for take-home testing in Aim#4	-
7.2	Walk & Run	• Walking and running on a flat paved trail with an inactive ankle increased the intensity	• Same as treadmill test results (6.1 above (Fig. 2)), supporting the consistency of the	-

		of the bending strain signal compared with an active ankle	observation	
8.1	Run	• New variable stiffness strut design tolerated running	• Improvements solved the strut deformation problem	-
8.2	Run	• Little change in magnitude of bending strain for low stiffness vs. high stiffness strut for the active ankle condition, but more substantial changes for the inactive ankle condition. Changes were greater for walking uphill than on a flat surface	• The results we are collecting on able-bodied participants with an active ankle may not reflect results for a person with ankle disability • The adjustable stiffness strut may have greater beneficial impact on uphill terrains than flat surfaces	Fig. 3
8.3	Run	• Stance phase duration expressed as a percentage of step duration was higher for the low stiffness strut compared with the high stiffness strut	• Stance phase duration should be considered as a controller feedback variable	Fig. 4
9.1	Walk & Run	• The participant was able to walk and run with accentuated hip/knee flexion and accentuated hip/knee extension	• It is possible to execute studies on able-bodied participants to simulates flexion/extension gait adaptations	-
9.2	Run	• The percentage of a step spent in stance phase was greater at high knee flexion and lowest at high knee extension	• Timings variables should be explored to understand disabled participant gait adaptations	Fig. 4,5
9.3	Walk & Run	• The magnitude of the bending strain signal changed for high knee flexion and high knee extension compared with normal for walking, but not for running	• Findings for walking are not directly applicable to running	Fig. 4,5
9.4	Walk	• The shape of the bending strain signal, i.e., timing variables, changed for a low stiffness v. a high stiffness strut, whether at high knee flexion, high knee extension, or normal	• Timing of bending strain events (e.g., maxima) may be a more appropriate feedback control variable than bending strain magnitude	Fig. 6
10.1	Run	• Adjustments to DAFO ankle angle were made – plantarflexed (7°), neutral (0°), dorsiflexed (7°) – while the participant ran on slopes of comparable angle. Participant attempted to simulate one type of lower limb disability (ankle fusion) by making his ankle stiff and at the same time relaxing the distal portion of his foot	• The adjustment mechanism performed as designed and executed appropriate angle changes	-
10.2	Run	• The timing of the maxima in the bending strain data was similar among “matched” conditions, e.g., plantarflexion for downhill, but not “mismatched” conditions	• Designing the controller so that it maintains consistent timing of the bending strain stance phase maxima may effectively accommodate changes in terrain slope	Fig. 7
10.3	Run	• Loading rate (change in bending strain per unit time) was more consistent for mismatched conditions than matched conditions	• Participant may have felt unstable in the mismatched conditions and thus focused on maintaining consistent loading and unloading rates	Fig. 8
11.1	Run	• Different strut stiffnesses were tested. The protocol was stopped between settings to manually make the adjustments • Minimal difference in the bending strain signal was observed for different strut stiffness settings	• Consistent with earlier results (8.2), there was little difference in bending strain magnitude • The motorized adjustment mechanism must be used to conduct plant gain testing because the delay between trials may mask the relationships between strut stiffness adjustment and changes in the bending strain signal	-
12.1	Run	• Bending strain magnitudes for three PDE struts (3, 5, 7) showed little change in bending strain magnitude, consistent with the 11.1 result	• Use of the adjustable stiffness strut design was likely not the reason for the 11.1 result	Fig 9
13.1	Walk	• Motor-driven adjustable stiffness strut used during continuous walking	• Adaptations to gait were much easier to identify than previously, suggesting it will be possible to collect good plant gain data	-

			on participants	
14.1	Walk & Run	• Using IMUs to track ankle angle performed well but an alternative strategy is needed for data storage	• An I^2C version of the IMU is needed	-
15.1	Run	• Plant gain (Pltgain) protocol for strut stiffness produced a measurable gain (i.e., there was a linear relationship between the bending strain maxima and strut spacing) but relatively large strut stiffness changes need to be made. A measurable slope was also recorded for strut spacing plotted against the timing of the bending strain maxima as a percentage of step duration, but the change was small	• Use of the IMUs should be pursued as an alternative feedback control variable to bending strain	Fig. 10
Participant F-2				
1.1	Run	• Participant able to run comfortably • Participant had difficulty running comfortably while attempting to relax the ankle	• Participant included in study, but may have difficulty simulated a person with lower limb disability	-
2.1	Run	• Strain-gage signal saturation issues – amplifier gain adjustments required	• Signal is sufficiently strong for the need, thus the footplate thickness is acceptable	-
3.1	Run	• The shape of the bending strain waveforms was comparable to that for participant F-1	• Consistency suggests proper performance of the instrumentation	-
Participant F-3				
1.1	Run	• Participant able to run comfortably but did not feel a stiffness adjustment. The Al strut was too thick for this participant. The max and min stiffness of the strut need to be reduced • Participant had difficulty running comfortably while attempting to relax the ankle	• Participant included in study, but a thinner Al strut will be needed	-
2.1	Run	• Thinner Al strut produced an acceptable stiffness range	• Participants may need different stiffness ranges – probably depends on their height, weight, shoe size, and running mechanics	-
3.1	Run	• Strain-gage signal saturation issues – amplifier gain adjustments required	• Signal is sufficiently strong for the need, thus the footplate thickness is acceptable	-
4.1	Run	• The shape of the bending strain waveforms was comparable to that for participant F-1	• Consistency suggests proper performance of the instrumentation	
5.1	Run	• While being adjusted during running, the strut stiffness adjustment assembly failed	• Having the adjustment assembly protrude outward posteriorly is inappropriate because of the high bending strain induced at the connection to the strut. Design needs to be modified accordingly	
Participant F-4				
1.1	•	• Participant able to run comfortably • Participant had difficulty running comfortably while attempting to relax the ankle	• Participant included in full study, if needed	

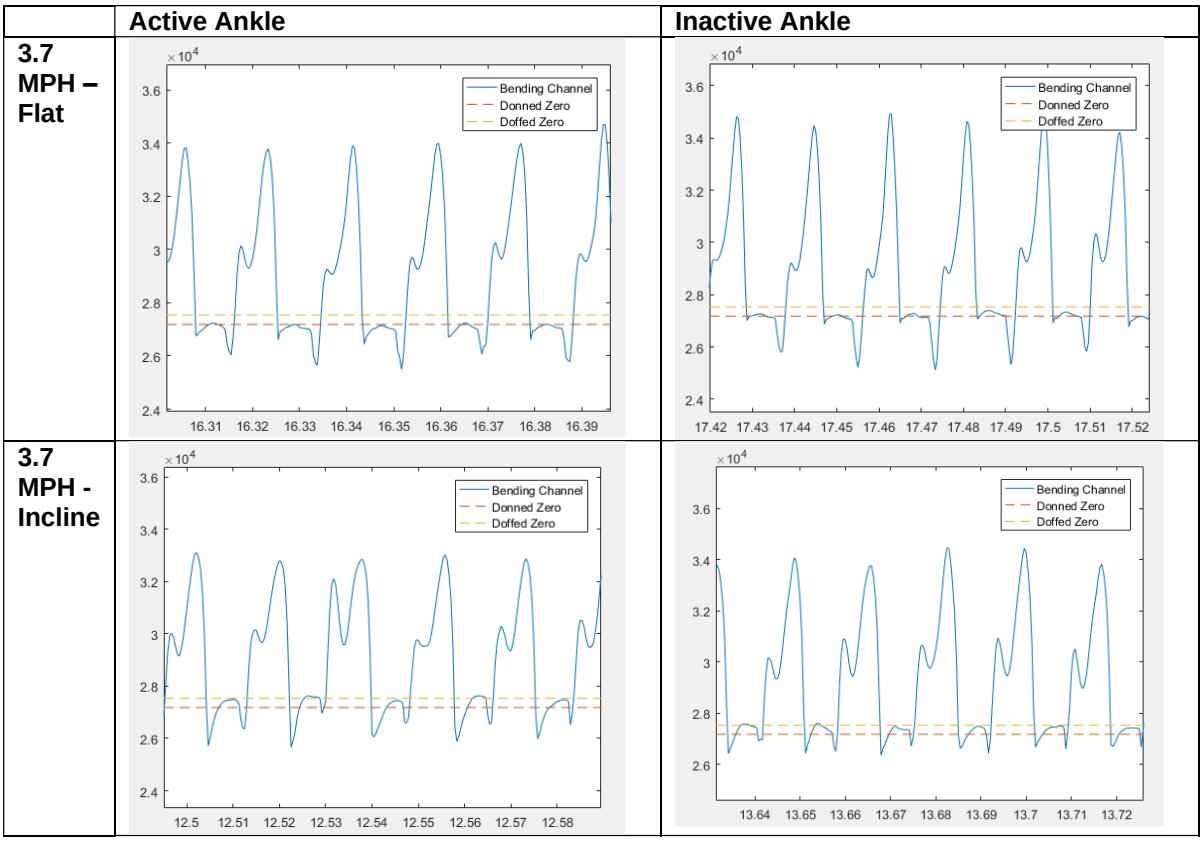

Fig. 2. Walking results. The data above shows walking data from the bending strain gages mounted on the footplate. The signal peaks show maximum footplate bending from plantarflexion at push-off, while the valleys show action of the heel lever arm during early stance phase. The donned and doffed zero lines show the baseline strain gage value under no weight bearing before and after the participant donned the DAFO. They are not of identical magnitude because presence of the participant's limb deformed the DAFO. These results show that the peak bending strain increases when the ankle is inactive vs. active, and the first peak becomes more apparent when an incline is introduced.

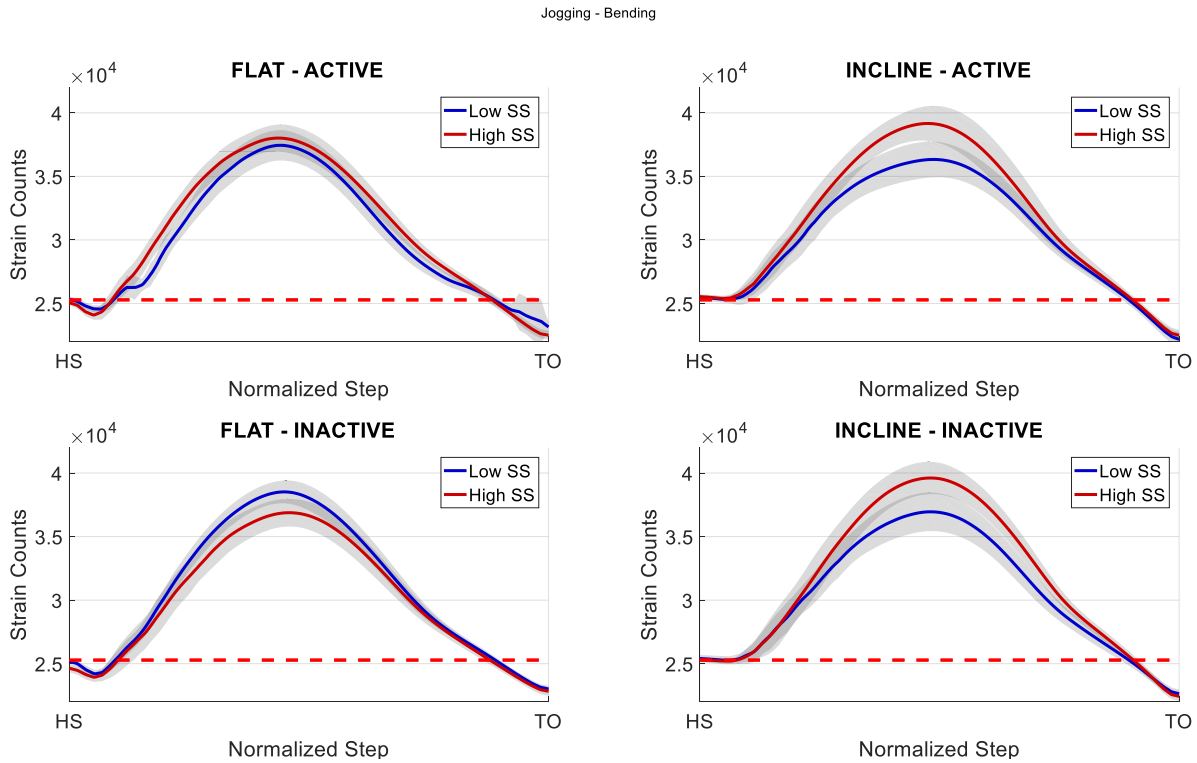

Fig. 3. Jogging results – stance phase only – for low and high strut stiffness (SS). The data above represents an average taken of a series of steps represented as a single step waveform with step-to-step variability represented by the grey shadows outlining the colored averaged

line. This presentation is helpful towards illustrating timing differences under different test conditions, aiding in the identification of metrics for the controller algorithm. Differences were more accentuated for the inactive than active ankle. Differences were more accentuated on an inclined than flat surface.

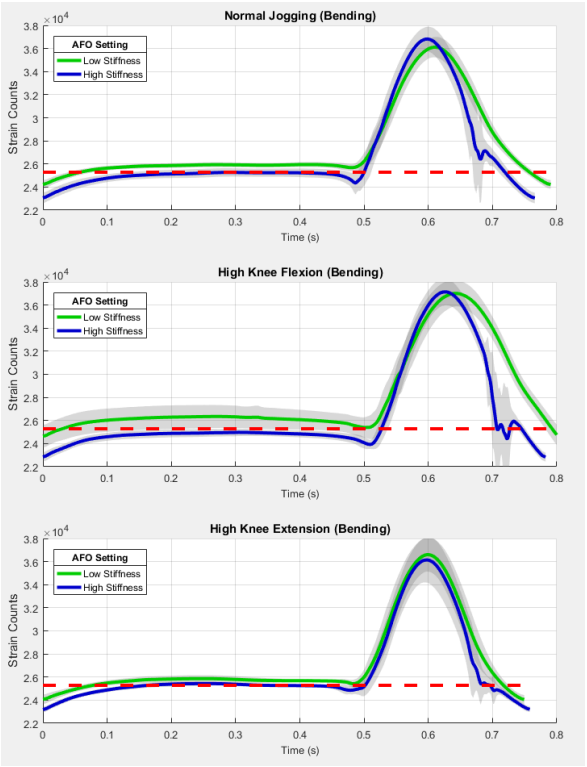

Fig. 4. Jogging results for normal, high knee flexion, and high knee extension. The shape of the bending signal was affected by a change in strut stiffness, while the peak magnitude remained consistent.

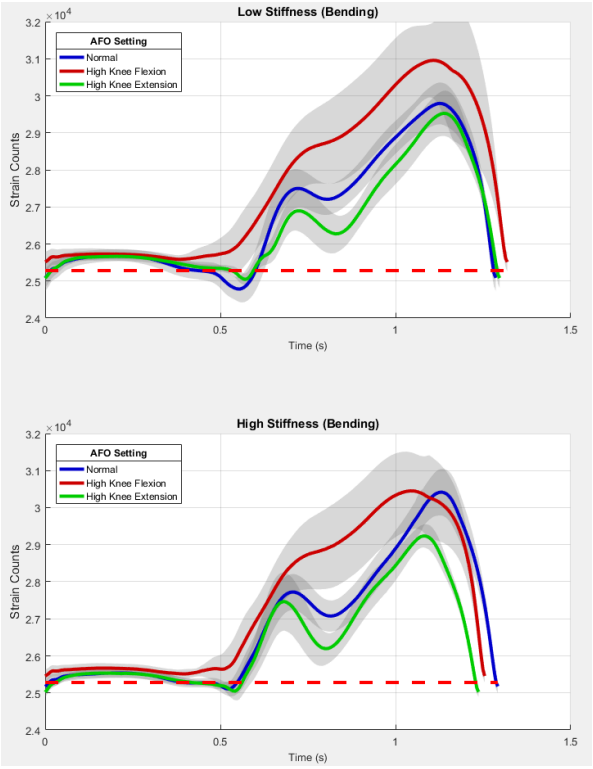

Fig. 5. Walking results for normal, high knee flexion, and high knee extension. The magnitude of the bending signal was affected by knee action whether a low stiffness or a high stiffness strut was used.

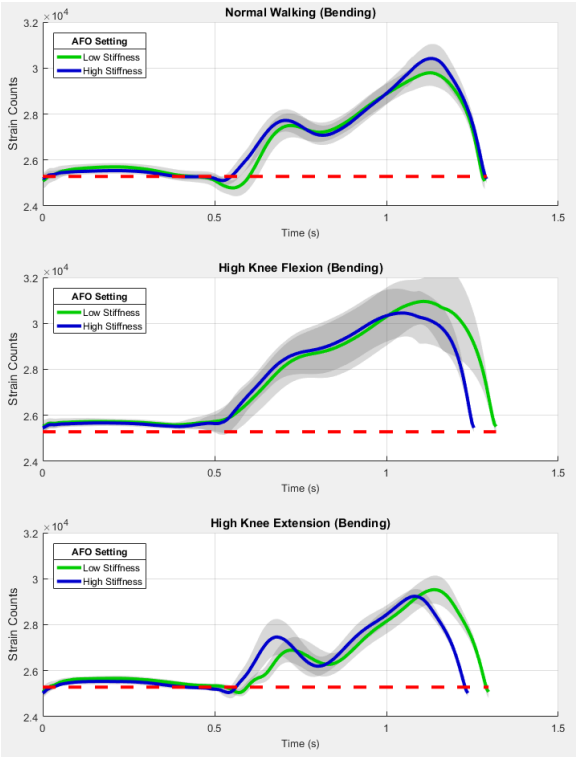

Fig. 6. Walking results for a change in strut stiffness for normal walking, high knee flexion, and high knee extension. The shapes but not the magnitudes of the bending signal data were affected by strut stiffness.

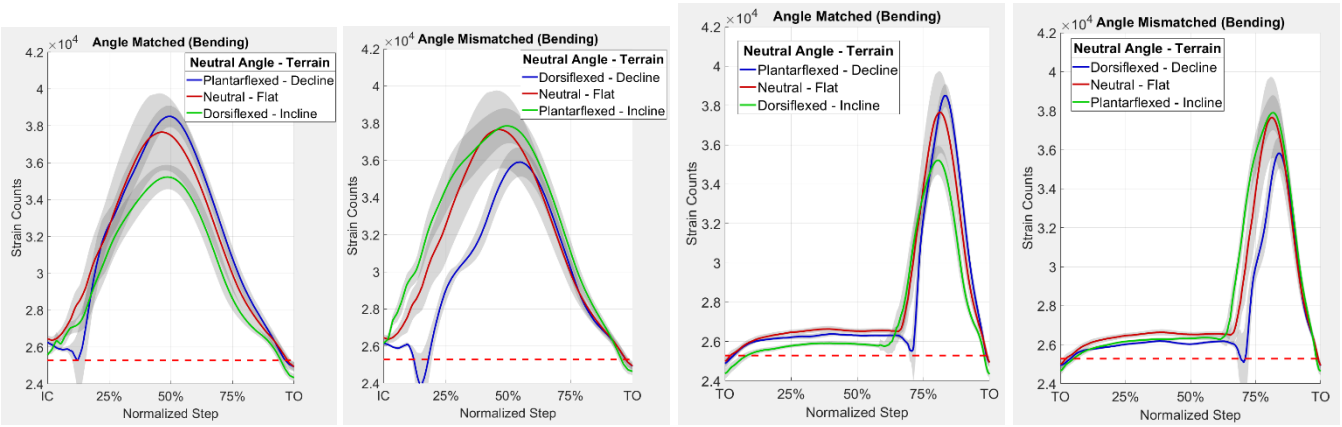

Fig. 7 (left). Stance phase results from running with different DAFO angles on different terrains. (a) DAFO angle adjustment and terrain are matched. (b) DAFO angle adjustment and terrain are mismatched.

Fig. 8 (right). Stride results highlighting loading rates. (a) For the matched conditions, there are a range of loading and unloading rates. (b) For the mismatched condition, loading and unloading rates are more consistent.

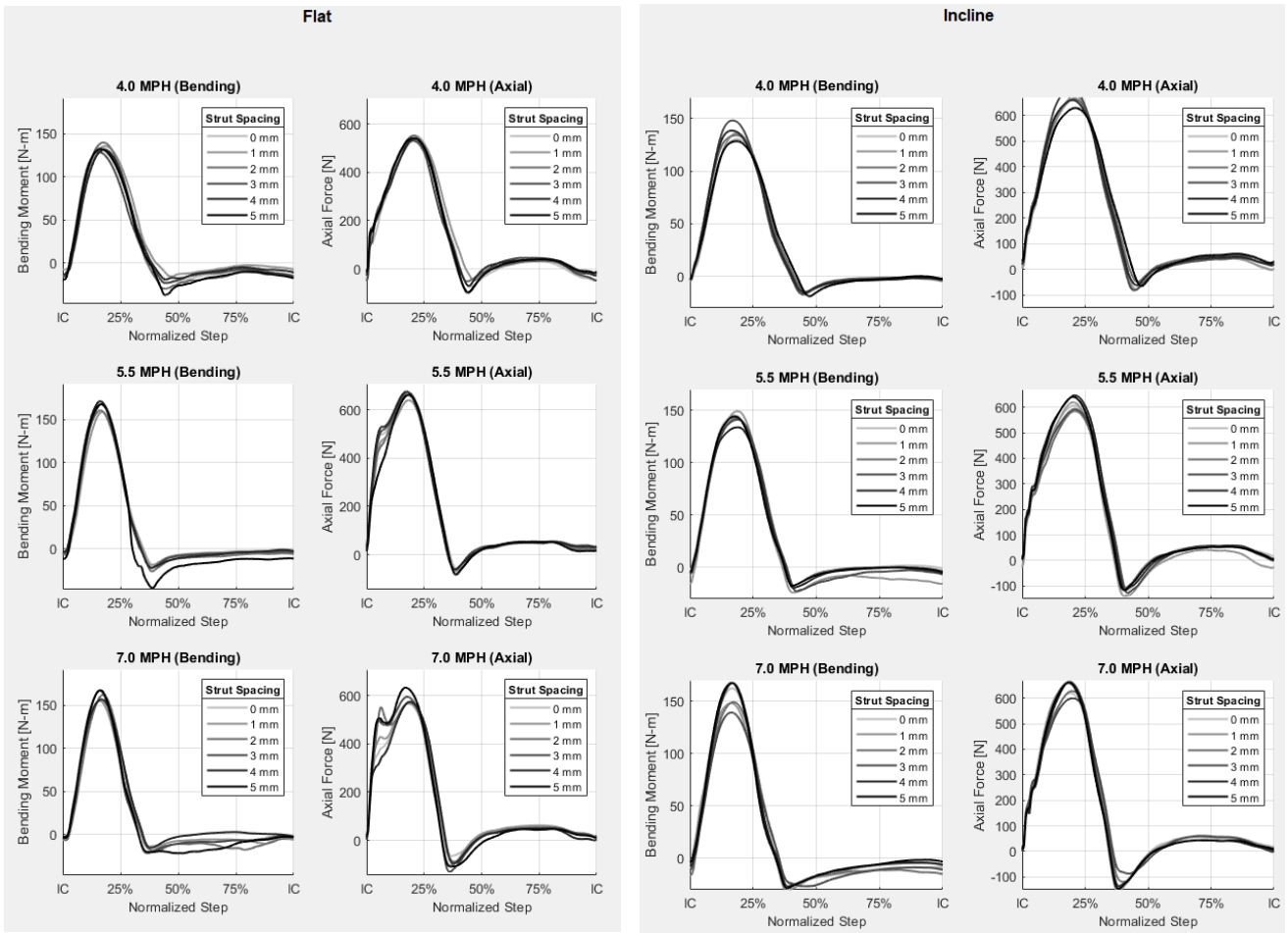

Fig. 9. Footplate bending strain and axial strain results for different strut stiffness settings. The legend indicates the strut separation distance. A higher distance corresponds to greater strut stiffness. In general, magnitude differences for different strut stiffnesses were low.

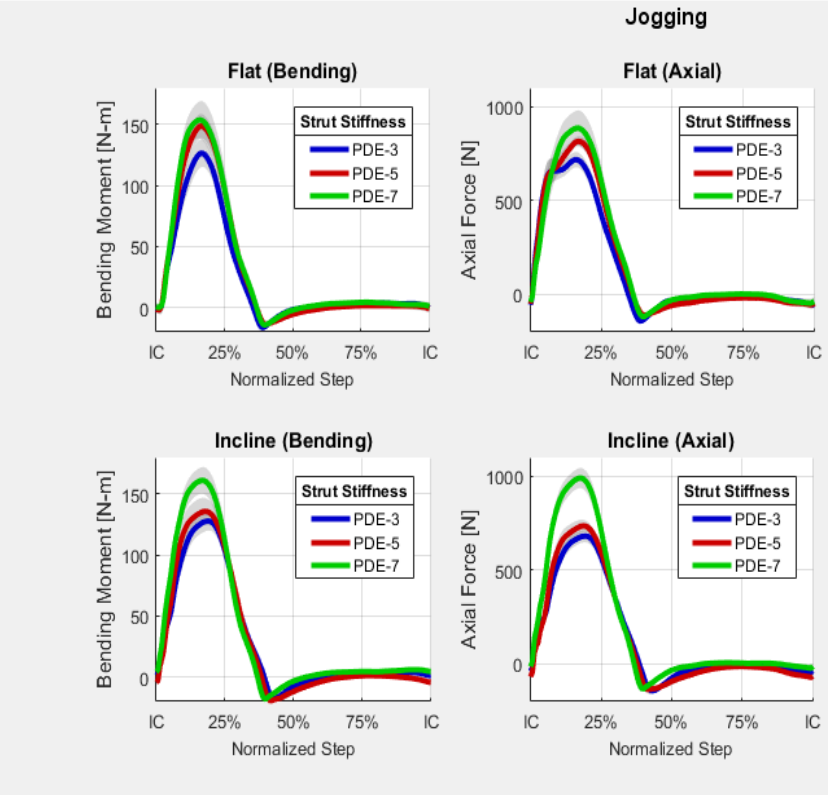

Fig. 10. Footplate strain gage results using a PDE strut instead of the adjustable strut. The running speed was 5.5 mph. Changes in the signal are visible, but this may be because the adjustment range was large, 4 PDE levels.

Results from the studies described above led us to conclude that the variables running speed and surface terrain slope are the most likely environmental variables to affect the measurements of interest. The measurements of interest are the candidate metrics to be used in the auto adjustment system. They include stance phase maxima of: footplate bending strain magnitude and timing, footplate axial strain magnitude and timing, and DAFO deflection and timing. Ankle activity and knee angle are the most likely user action variables to affect the measurements of interest. Strut stiffness and DAFO angle (pflex/dflex) are the variables in the DAFO that we control. The variables and how they are expected to affect the measurements of interest across all participants are summarized in Table 4.

Table 4. Variables Hypothesized to Demonstrate an Approximately Linear Relationship with the Measurements of Interest. Hypothesized based on results from test results summarized in Table 3.

Type	Variable	Peak bending strain		Peak Deflection	
		Magnitude	Timing	Magnitude	Timing
Environmental	Running speed	X	-	X	-
	Surface terrain slope	-	X	-	X
User Action	Ankle activity	X	-	X	-
	Knee angle	-	X	-	X
Controlled	Strut stiffness	X	-	X	-
	DAFO pflex-dflex	-	X	-	X

To test the hypotheses listed in Table 4 and determine the necessary information to begin programming the automatic adjustment system, we developed 3 testing protocols. Brief descriptions of each protocol are below. Detailed protocol documents are included in Appendix 1. Results from execution of the protocols on participants F-1 to F-3 are described below.

In addition to generating the hypotheses listed in Table 4, the results from the studies described above led us to execute a series of tests using an ankle foot testing system (AFT), a machine that we custom designed with a collaborator as part of a prior project. The AFT is a gait simulation machine that allows us to program both the force and direction of load delivery to be applied to the DAFO. This system allowed us to isolate variables affecting performance, and better modify the design and instrumentation to meet the project needs. Results from AFT testing are described in the *Engineering* section in the latter half of this report.

The 3 test protocols executed on all able-bodied participants include:

- *Stiffness-Gait:* Participants perform running trials on the treadmill, attempting to keep their ankle inactive. Two strut stiffness settings are tested, nominal and deviated. The participant performs trials at 3 speeds, walking, nominal running, and 50% faster than nominal running, and 3 different knee actions during stance phase, nominal, heightened flexion, and heightened extension. Part of the basis for including knee action is that in gait analysis research studies reported in the literature, knee angle adjustment was suggested a compensatory mechanism when participants ran wearing different stiffness DAFO struts [Clin Biomech 2015;30:1125-1132]. Two additional trials are performed with the ankle active. There are 10 conditions altogether (not all possible combinations of variables are tested). The purpose of this test is to identify the dominant variables, among strut stiffness, cadence, knee action, and ankle activity, that affect the monitored variables (footplate strains; DAFO deflection). We use cadence instead of speed because in the portable auto adjusting DAFO, we will not monitor speed, only cadence. For the monitored variables, both magnitude and timing of maxima are explored in analysis. We also quantify the time percentage of a step that is stance phase (stance phase percentage).

- *Ankle Angle-Outdoor Terrain:* Participants perform walking and running trials outdoors on a trail near the lab. DAFO angle is adjusted to plantarflexed, nominal, and dorsiflexed settings. The participant performs these trials on 3 different surface inclines: flat, uphill, and downhill. Thus, there are 18 conditions altogether (2 speeds, 3 angles, 3 inclines). The purpose of this test is to characterize how the monitored variables (footplate strains; DAFO deflection) change when the ankle adjustment is matched and not matched to the surface terrain slope.

- *Plant Gain-Treadmill Terrain:* Participants perform a running trial on the treadmill while strut stiffness is adjusted across its adjustment range. Participants perform a second trial identical to the first but with the running surface at an incline of 10% grade (5.7°) instead of flat. Results establish the plant gain value for the user for use in the auto adjusting system. Insight is gained into if a different plant gain value will be necessary in the controller for incline running. We recognize that it may be necessary to also test on a downhill grade. However, our current treadmill lacks that capability. If out-of-lab testing demonstrates different results for downhill vs. uphill, then equipment elsewhere will be used to test at all 3 grades: 0%, 10%, -10%.

Results from the 3 tests protocols on able-bodied full study participants

In the results presented below, footplate data are shown in units of strain gage counts. Strain gage counts are proportional to bending moment magnitude, as demonstrated during calibration testing. We use strain gage counts in the plots because the automated adjustment system, which is programmed into a microcontroller mounted on the DAFO, operates using these units. Conversion to other units would add an additional unnecessary computational step, reducing efficiency in the microcontroller.

One test was run on each participant for each of the three protocols. Results discussed below were consistent for all 3 participants unless otherwise stated.

Stiffness-Gait

For all able-bodied participants, using an active ankle affected our independent variables of interest. Actively firing ankle plantarflexors reduced peak bending strain (in the footplate) and DAFO deflection (measured cuff-footplate angle) (Fig. 11). Pushing down at the metatarsals countered action of the DAFO. The magnitude of this effect was larger during walking than running, possibly because passive ankle forces were larger during running, reducing impact of the active ankle contribution to the signals. Based on the consistency of the result, in subsequent testing participants were instructed to try to eliminate their active ankle contribution in all trials.

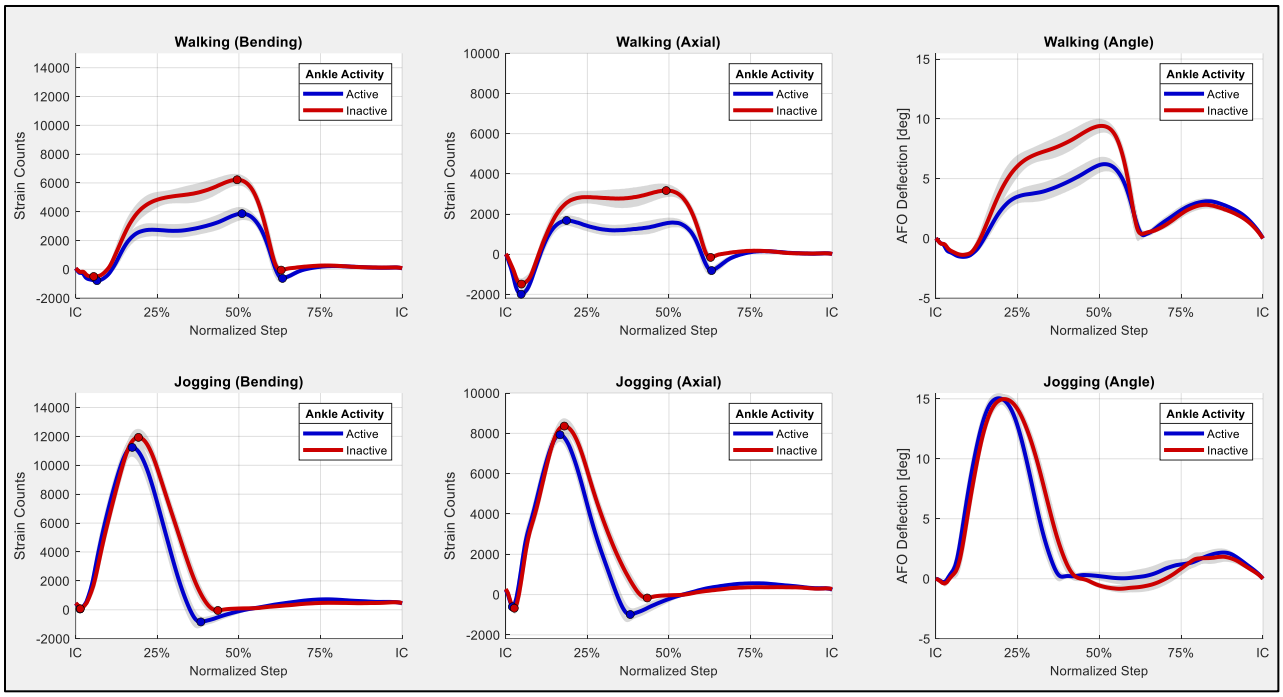

Fig. 11. Walking and running (jogging) results – impact of ankle activity on footplate strains and DAFO deflection. Example results from participant F-2 are shown. The participant's active plantarflexion reduced the bending and axial strain magnitudes in the footplate and the DAFO deflection measured by the IMUs.

For both high and low strut stiffness conditions, intentional changes in knee activity had measurable effects on both bending strain and DAFO deflection, consistent with results from the earlier tests listed in Table 3. Running with exaggerated knee flexion increased peak bending strain, DAFO deflection, and stance phase percentage (Fig. 12), also consistent with Table 3 results. The increased bending strain may reflect a higher resultant force applied at the footplate, or the resultant force being applied further out towards the toe. Running with exaggerated knee extension had the opposite effect – decreases in peak bending strain, DAFO deflection, and stance phase percentage. The reduced deflection and stance phase percentage are consistent with the interpretation that participants attempted to offload the DAFO limb when exaggerating their knee extension, possibly to minimize discomfort, or possibly because the third rocker action occurred earlier and forced an earlier weight transition to the contralateral limb. In the example data shown in Fig. 12, peak bending strain occurred earlier during stance under exaggerated knee flexion and later under exaggerated knee extension, but this observation was inconsistent across participants. We did not observe a consistent trend across participants of a stronger or weaker dependence at one strut stiffness over another.

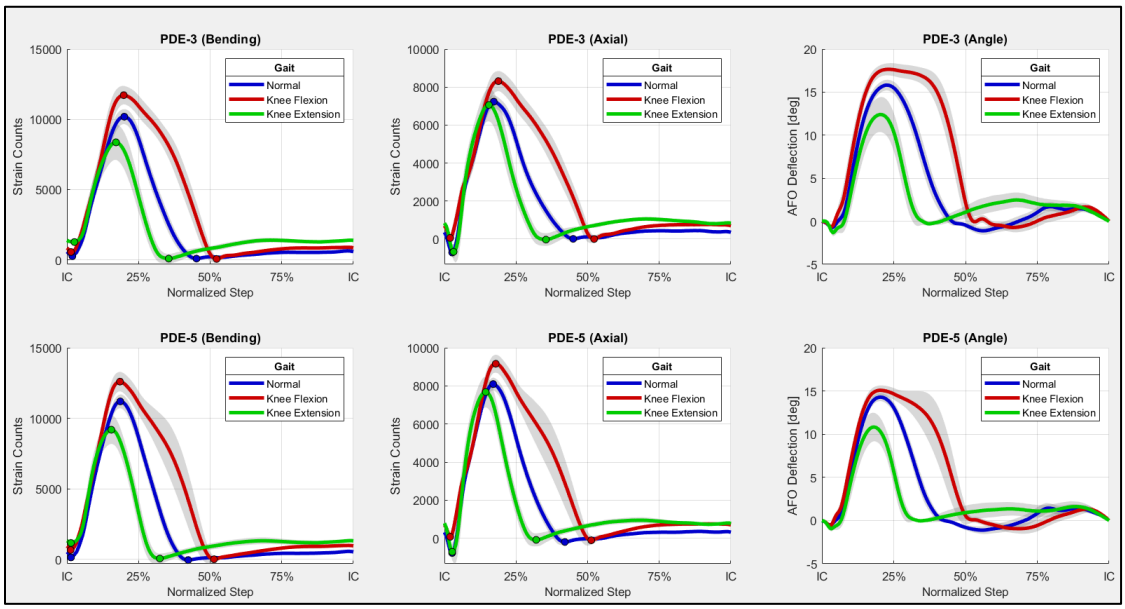

Fig. 12. Stiffness-Gait testing protocol – effects of knee action on footplate strains and DAFO deflection. Example results from

participant F-2. Exaggerated knee flexion increased peak bending strain, DAFO deflection, and stance phase percentage. Exaggerated knee extension had the opposite effects.

For all participants, increasing running speed increased peak bending strain, axial strain and DAFO deflection, and reduced stance phase percentage, consistent with expectation (Fig. 13). We did not observe across participants a stronger or weaker dependence at one strut stiffness over another.

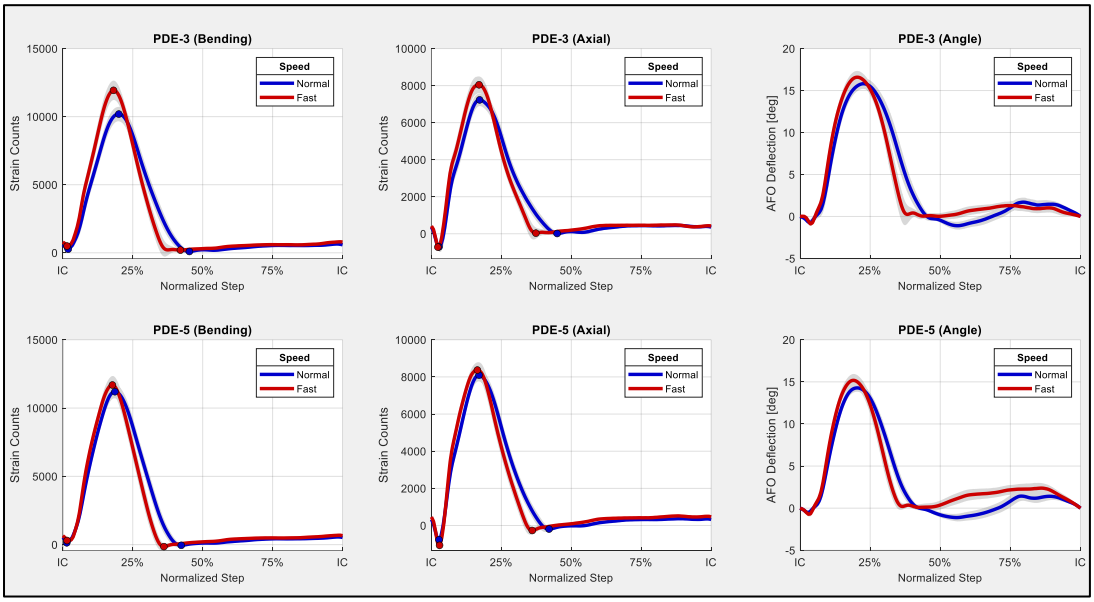

Fig. 13. Stiffness-Gait testing protocol – effects of running speed. Increasing running speed increased the bending strain, axial strain, and DAFO deflection.

These results provide insight into how we might expect the variables of interest to change on participants with ankle disability. For example, if a participant reduced his or her stance phase percentage at a given cadence, this may indicate that the DAFO is too compliant for the current situation and the person is employing heightened knee extension as a compensatory mechanism.

The dependence of some of the metrics of interest on running cadence suggests that cadence is a meaningful environmental disturbance and is relevant to operation of the auto adjusting system.

Ankle Angle-Outdoor Terrain

Matching DAFO angle to terrain angle resulted in consistent peak bending strain timing, loading and unloading rates compared to the mismatched conditions (Fig. 14). “Matching” means that the direction of DAFO angle adjustment matches the direction of slope of the running surface. When the DAFO was overly plantarflexed for the uphill terrain, the peak bending strain increased and occurred earlier within stance phase. When the DAFO angle was overly dorsiflexed for the downhill terrain, the peak bending strain decreased and occurred later within stance phase.

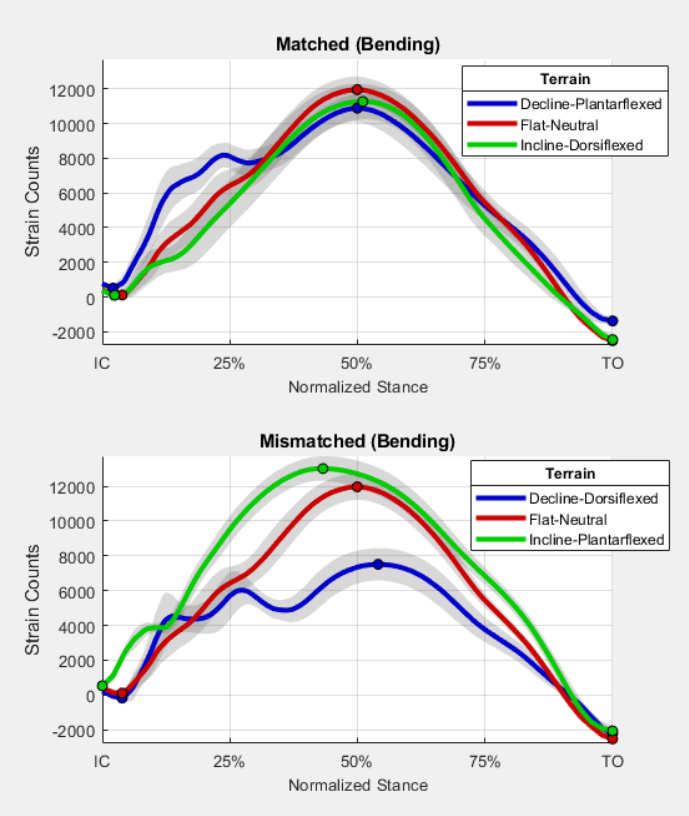

Fig. 14. Ankle Angle-Outdoor Terrain testing protocol – effects of DAFO angle and slope of the terrain. Example results from participant F-2. The bending strain result was relatively consistent when the DAFO angle was matched to the surface terrain (upper graph) and not consistent when it was mismatched (lower graph).

Timing of the peak bending strain was consistent for the matched condition across participants, however, magnitude of the peak bending strain was not. For two participants, peak bending strain for the decline-plantarflexed condition was of lower magnitude than for the flat and incline-dorsiflexed conditions (data not shown).

The results suggest that the timing of the peak bending strain should be used as a fit metric in the controller to adjust the DAFO angle when a participant runs on surfaces of varying incline. This result is consistent with the operational design of powered prosthetic ankles worn by people with lower limb amputation. Gait timing variables are used to determine adjustment. However, we are using bending strain data in the footplate for this measurement instead of other sensors.

Plant Gain – Treadmill Terrain

During a plant gain test, conducted in the lab on the treadmill, the adjustment variable (strut stiffness or DAFO angle) is gradually changed, using the motor-driven mechanisms (Fig. 1a,b), over its range while all other variables are held constant. Because development of the adjustable stiffness strut was slowed (see *Engineering* section below), we executed abbreviated plant gain tests on the 3 able-bodied participants (F-1 to F-3). The participants ran on the treadmill wearing PDE struts of 2 different stiffness (PDE-3, PDE-5), stopping between tests so that the researcher could swap out the PDE strut.

The abbreviated version of the plant gain test for DAFO angle was identical to data collected during the ankle angle-outdoor terrain protocol described above, except that the ankle angle-outdoor terrain protocol was more complete. It included results for 3 terrain slopes instead of just 2. The DAFO angles used were 0°, -7.5°, 7.5° for flat, plantarflexed and dorsiflexed, respectively. The 3 terrain slopes were 0°, -7.5°, 7.5° for flat, downhill, and uphill, respectively.

Consistent with the hypothesized results listed in Table 4, these data indicate that the most sensitive metric for strut stiffness is the peak DAFO deflection magnitude (PDM), and the most sensitive metric for DAFO angle is the percent peak bending strain timing (BST) as a percentage of stance phase. Both running speed and knee action introduced meaningful disturbances to the PDM metric (Fig. 15,16), though the running speed perturbation produced more linear results – the 2 lines in each of the 3 plots are approximately parallel with each other. Parallel lines indicate that the plant gain, the slope of the line, is consistent. This result strongly supports the expectation that the controller will properly manage strut stiffness to changes in running speed and maintain a consistent DAFO deflection. The 3 lines in the knee action data are not parallel; some of the lines cross (Fig 16). The knee action effort, however, was a forced adaptation, thus the relevance of this result towards control system performance is unclear. At this point, we can say that user knee action may be a relevant variable that affects the PDM in a complex way. It

is possible that other metrics will allow us to distinguish knee action from other disturbances if knee action data needs to be incorporated into controller operation (unlikely). Surface terrain had a meaningful impact on the BST metric (Fig. 17), as expected. The non-linearity in the plot may be a result of the sitting period between trials, knee action adaptations made by the participants to improve comfort, or something else. Data collection using the motor driven DAFO angle adjustment mechanism will help clarify the source of non-linearity. It is possible that the IMU-measured peak DAFO deflection matches timing of the peak bending strain and thus may replace that measurement, eliminating the need for the strain gages and thus simplifying the instrumentation. This possibility will be investigated in Year 3. Because users of the auto adjusting DAFO will be people with lower limb disability, the influence of user ankle action is not relevant thus was not plotted here. Overall, the results shown in Fig. 15 to 17 are very encouraging.

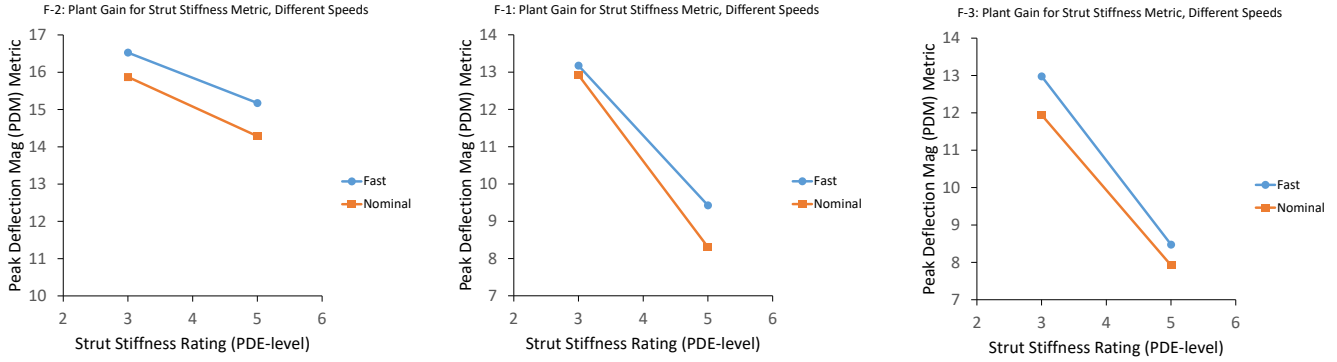

Fig. 15. Plant gain results for strut stiffness - running speed introduces a meaningful disturbance. The line shifts up at a faster speed, indicating an elevated PDM metric. Data for participants F-2, F-1, and F-3 are shown.

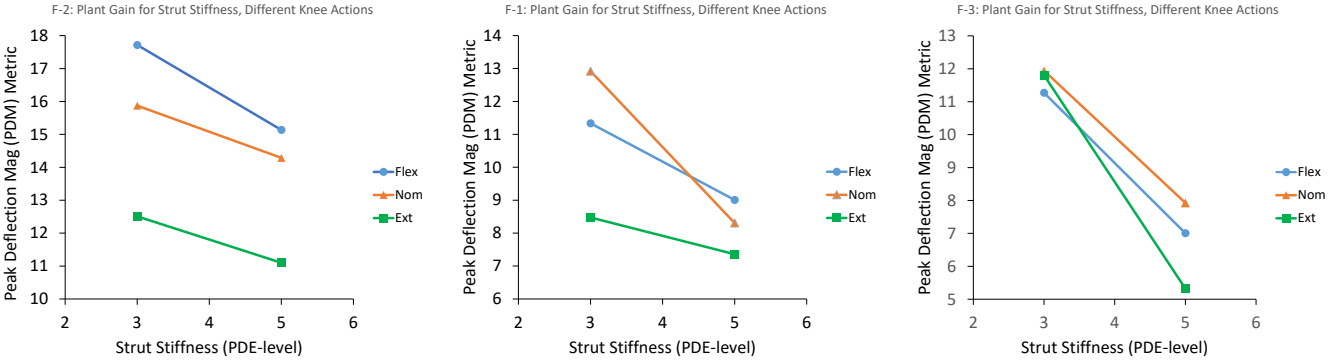

Fig. 16. Plant gain results for strut stiffness - knee action introduces a meaningful disturbance. The line shifts but not always linearly with strut stiffness. Data for participants F-2, F-1, and F-3 are shown.

Fig. 17. Plant gain results for DAFO angle (in degrees) – surface terrain slope introduces a meaningful disturbance. Data for participants F-2 and F-3 are shown. Data were not available for participant F-1.

Control system diagrams that we generated based from these data are illustrated in Fig. 18a for strut stiffness and in Fig. 18b for DAFO angle. The "metric" (*y*-axis) is the measured signal that will be controlled in the auto adjustment system. The controller seeks to maintain a consistent set point that we specify for the metric. If the relationship between the metric and the

variable is linear, then a proportional-integral (PI) control system is implemented. If the relationship is non-linear then a proportional-integral-derivative (PID) control system is necessary.

The parallel diagonal lines in the control system diagrams indicate the path the control system will take to bring the PDM and BST back to the set points. For strut stiffness, consider a participant who starts at point A on the diagram. The PDM is at the set point, so no adjustment is made. Then there is a perturbation – the person starts running at a faster cadence, for example. The PDM metric increases to point B. The control system is activated in response to the change in PDM and increases strut stiffness, moving to point C in the diagram. The controller stops adjustment when the set point is reached. At some time later, there is another perturbation – the person slows down. The PDM metric decreases to point D. The control system responds to the change in PDM and decreases strut stiffness, moving to point E in the diagram. The controller stops adjustment when the set point is reached. The controller response strategy is similar for the BST metric / DAFO angle plot (Fig. 18b), except that the slope is positive and thus that path is in the opposite direction.

There are other possible perturbations besides running speed and knee action that may affect the PDM and BST metrics. For example, the hardness of the surface terrain may be a meaningful disturbance. It is important to note that the control system should not need to be calibrated to each type of disturbance. We selected what we considered the most meaningful ones to investigate in participant studies discussed above to test how the disturbance changes the selected metrics. If the PDM and BST metrics correctly monitor clinical fit, then the system should respond properly to any perturbation.

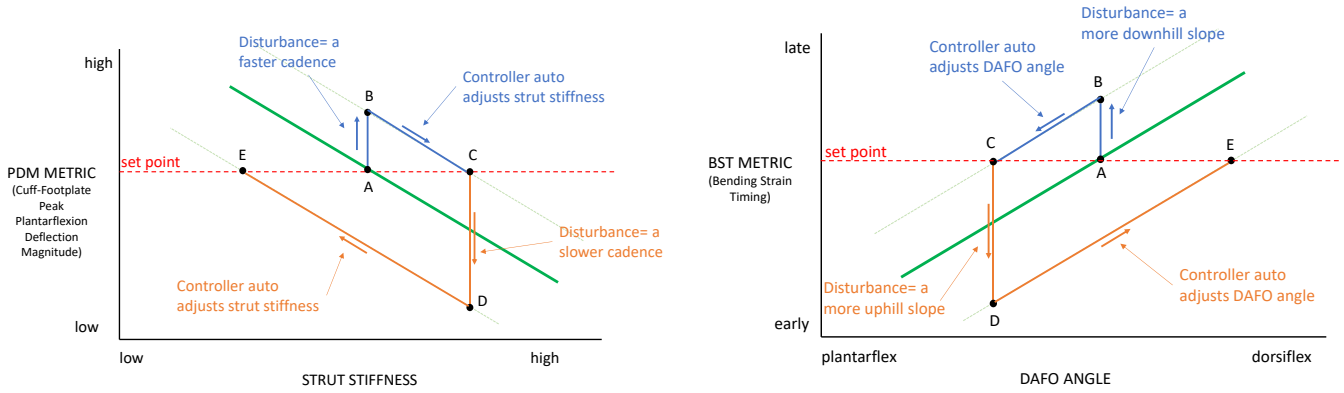

Fig. 18a,b. Controller diagrams for (a) strut stiffness and (b) DAFO angle. These diagrams illustrate how the control system will adjust when a disturbance is introduced.

Engineering

The adjustable stiffness strut system was updated to include: the design of a motor assembly that electronically changes the strut stiffness, minor modifications to the struts and their support hardware to overcome performance issues identified during participant testing, and a separate motor assembly that electronically adjusts the DAFO angle. Sensor and electronic updates included the design of a new clamping system to ensure strain gages were under a constant pressure during curing, the replacement of numerous strain gage circuit wires with flexible circuit boards affixed to the footplate, the incorporation of IMUs into the cuff and footplate assemblies for DAFO deflection measurement, and the design of new housings for the signal conditioner and data acquisition circuitry.

Double Strut – Updated Mechanical Design

Addition of motor assembly to electronically change strut stiffness

We incorporated a motor and connection to a laptop to control the stiffness in the adjustable strut system. The motor changes the spacing between the Al and carbon fiber struts, pulling the rear carbon fiber strut outward or pushing it inward. Pulling out the rear strut increases the moment of inertia of the entire system at the height where the strut bends. This change increases the overall stiffness of the system.

The first iteration of this design (Fig. 19a) effectively changed stiffness, accomplishing a strut stiffness range of PDE-4 to PDE-7. Based on our clinical experience, it is unlikely that a single participant will need a stiffness adjustment of more than 3 PDE levels when transitioning from walking to running. However, the design failed during participant running tests because of the excessive bending moment induced by placing the heavy motor at the rear of the assembly. In the revised design (Fig. 19b), the motor is oriented vertically. The motor turns a 90° miter gear. The miter gear is attached to a lead screw that is mounted to the Al strut. This design brings the motor in closer, reducing the bending moment and improving the capability of the system to withstand load during running.

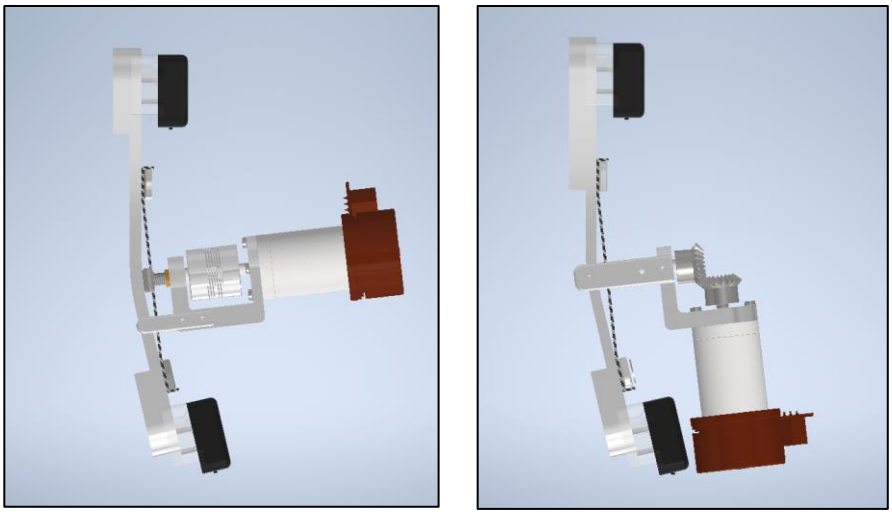

(a) **(b)**

Fig. 19a,b. Mechanism for electronic adjustment of strut stiffness. (a) In the initial design, the motor was oriented horizontally. (b) In the revised design, the motor is oriented vertically.

The motor-gearhead assembly selected was the lowest weight product found to supply at least 2 N·m of torque, the minimum necessary torque calculated during design, at 20 RPM. This torque is required to push the strut out near the furthest point in the adjustment range. The 20 RPM speed was needed to execute adjustment during the swing phase of gait. Adjustment during stance phase was not possible because it introduced a risk to participant gait stability and, in addition, would have required a stronger and thus heavier motor. If participant studies demonstrate that a lower torque will properly execute adjustment, then a smaller more lightweight motor will be used instead.

To execute a strut stiffness change, the lead screw displaces the single jack bar and pulls the carbon fiber strut away from the keyed aluminum strut, increasing the spacing (Fig. 20). The entire motor assembly is mounted to the aluminum strut via keys on the side. The keys limit displacement and thus minimize the vertical force delivered to the motor mount assembly during running. A parts list for the system is included in Appendix 2.

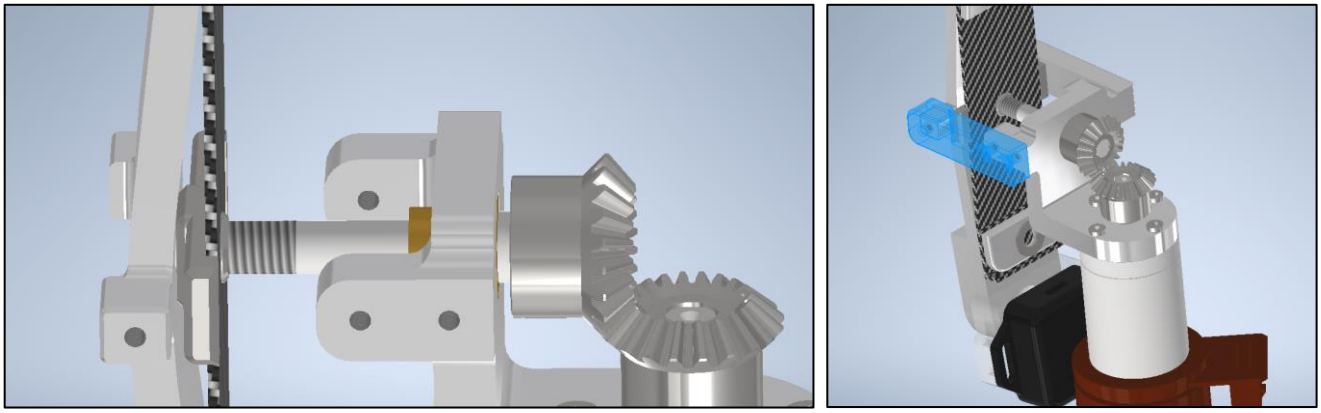

Fig. 20. Close up of the adjustment mechanism. To increase strut spacing, the lead screw displaces the single jack bar and pulls the carbon fiber strut away from the keyed aluminum strut.

The motor executes a 0.125 mm spacing adjustment between the two struts in 0.25 s. It applies a torque of 128 mN·m, stepped up to 8.4 N·m using a gearhead, to rotate the lead screw and raise the single jack bar, overcoming the stiffness of the carbon fiber strut. The minimum required torque was determined using a torque wrench to manually actuate the lead screw. We program in a higher torque of 8.4 N·m instead because inertial forces become relevant when we try to make adjustment quickly. The torque may be reduced later as we gain experience implementing the design. A summary of the motor assembly issues and modifications made is provided in Table 5.

Table 5. Engineering Design Changes Made to the Motor Assembly to Adjust Strut Stiffness

Issue	Modification Made
• During running, the motor applied significant load to the lead screw, causing unwanted bending of the lead screw and fatiguing the carbon fiber strut. This	• Miter gears were implemented to transfer torque from the motor to the lead screw, allowing the motor to be rotated 90 degrees downwards and reducing the moment arm of the loads applied to

happened because the motor was mounted perpendicular to the length of the strut, causing the weight of the motor to be applied over a long moment arm distance	the jacking bar and lead screw. Motor assembly is now rigidly fastened by keyed extrusions to the side of the aluminum strut, thus constraining vertical movement of the motor during running
• Main screw shaft too short	• The shaft length was updated as part of the change in motor orientation. The shaft needed to be longer so the motor would clear other parts on the DAFO
• Incorrect range of strut bending stiffness	• Al struts of different uniform thickness (4.5, 5.0, 5.5 mm) were fabricated to create double struts of different min and max stiffness
• The 4.5 mm strut plastically deformed during a plant gain test on a participant	• We incorporated 4-mm thick spacers into the mounting assembly at each end, strengthening the Al strut there and ensuring that it bends only in the middle

We hired a local manufacturer, Fiberdyne Labs, to manufacture the carbon fiber struts since consistency in fabrication is important towards our objective. The strut is about 110 mm in length, has a mounting hole at each end, and a middle hole for attachment to the adjustment mechanism (Fig. 21).

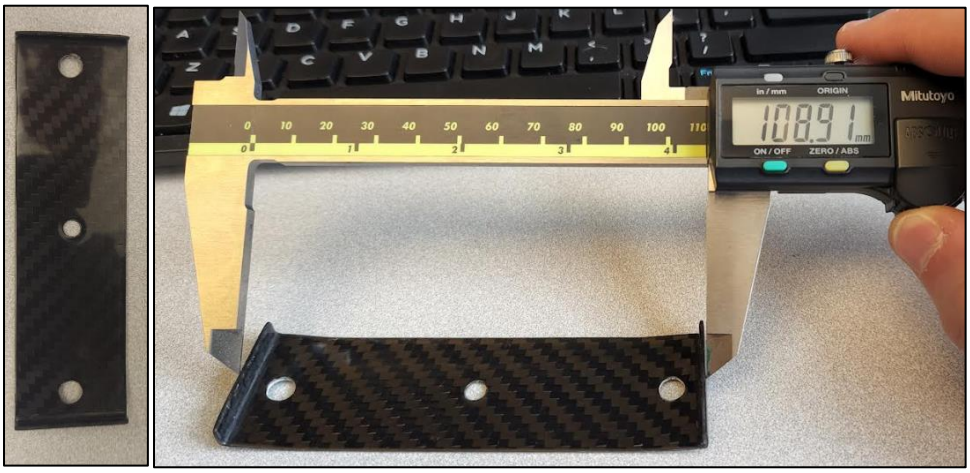

Fig. 21. Carbon fiber strut. We attempted to outsource manufacture this strut.

We underwent 3 design iterations with this manufacturer. Results and issues that arose are summarized in Table 6. We eventually needed to bring the fabrication process back in house and make the carbon fiber struts in our lab at the University of Washington.

Table 6. Fiberdyne Strut – Design Iterations and Performance

Design Iteration	Researcher comments, test results, and application to subsequent design
Fiberdyne 1	• Part inspection showed that the first iteration of carbon fiber strut prototypes did not meet design tolerances. Most critical, the overall length of the strut was too short and mounting holes were misaligned. We provided the manufacturer with revised drawings that highlighted the key dimensions • Stiffness of these struts was ideal as they were similar to the lab manufactured struts and were stiff enough to induce a stiffness change in the DAFO • Since the prototypes did not meet part tolerances, they had to be altered to fit into the DAFO assembly. As a result, stress concentrations were induced, and the prototypes fatigued quickly
Fiberdyne 2	• The second iteration of the carbon fiber strut overcame the dimensional accuracy problems • The size of the lead screw hole was increased to 8.1mm diameter to accommodate a larger lead screw in our motorized system • An error on the manufacturing floor resulted in a carbon fiber material change during the layup which drastically reduced the stiffness of the carbon fiber strut compared with the manufacturer's first iteration (Fig. 22). The new design was not viable for our application. The manufacturer believed that a different material was needed and attempted to use a new material in the next design iteration
Fiberdyne 3	• The third iteration of carbon fiber strut prototypes had tolerancing issues in hole placement and in addition was too compliant for our application. A trip to the manufacturer's facility revealed that the company was no longer in residence, i.e., ceased domestic operations. We moved carbon fiber strut manufacturing back to our lab
Lab-manufactured struts	• 3D printed molds were used to fabricate lab-manufactured carbon fiber struts • The struts were thicker than expected but the desired stiffness was achieved

• Further design changes are being considered to the shape of the molds as well as the material used

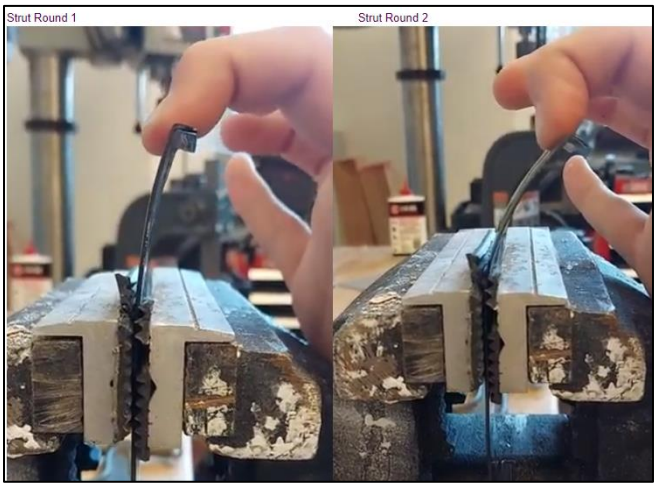

Fig. 22. Fiberdyne strut stiffness. The strut stiffness from the first iteration was acceptable (shown at the left). The strut stiffness from the second iteration was too low (shown at the right).

Minor modifications to double-strut mechanical design

While solving the manufacturing issues with the carbon fiber strut described above, we made several design modifications to the double-strut system. They are summarized in Table 7.

Table 7. Engineering Design Changes Made to the Double Strut Design

Issue	Modification Made
• During testing in the ankle-foot tester (AFT) (described below), we observed significant bending along the Al strut outside of the area covered by the carbon fiber strut. This limited the stiffness adjustment because the strut was bending in an area uncontrolled by the strut spacing	• This issue developed because there was a section along the top edge of the strut that was not well reinforced. To reduce bending in this area, we designed an extended spacer at the top attachment point, reinforcing the Al strut in this area and forcing bending to occur in the middle of the strut where stiffness was adjusted via the spacing between the two struts (Fig. 23)
• During assembly, the stiffness adjustment capability of the system was highly dependent on the torque applied to the carbon fiber strut mounting bolts	• In order to allow the carbon fiber to flex as needed during strut spacing adjustment without applying a significant pre-load to the Al strut, the carbon fiber mounting bolts needed to be as loose as possible. The bolts needed to constrain the location of the carbon fiber strut while allowing it to slip and bend as necessary during strut spacing adjustment. To accomplish this goal, the standard bolts used for mounting the carbon fiber strut were changed out for shoulder bolts with shims (Fig. 24). This design allows the stress applied to the carbon fiber strut during walking to be transferred to the upper and lower flange of the carbon fiber component • Maintaining a loose fit kept the materials within their elastic range, ensuring the carbon fiber strut returns to its original position when strut spacing is reduced
• While spacing between the two struts in the double-strut system determines the range of DAFO strut stiffness, the magnitude of the stiffness was determined primarily by the thickness of the Al strut. Our existing 4.5 mm Al strut accommodated a range of stiffnesses from PDE-3 to PDE-5. Thicker Al struts accomplish a PDE-5 to PDE-7 range	• To accommodate more lightweight participants who would typically use a PDE-1 strut for low intensity activity, a 3.75 mm thickness strut is needed. This thickness is difficult to fabricate. We are looking into metal versions of the rear strut that has similar properties to the carbon fiber strut
• Due to the limited accuracy we achieved fabricating the carbon fiber struts, the contact between the carbon fiber strut and the mounting plate which transfers load to the carbon fiber strut during walking was inconsistent. A lack of contact between the	• To improve the contact between the mounting plate and the carbon fiber strut, shims were adhered to the flanges of the carbon fiber strut. This modification transfers load from the Al strut to the carbon fiber strut more effectively, increasing the performance and the consistency of stiffness of the double-strut system

mounting plate and the carbon fiber strut resulted in no load being transferred to the carbon fiber strut, and the system was supported solely by the Al strut	
• Shims placed between the carbon fiber strut and aluminum strut sometimes fall out	• Adjustable mounting plates were designed so that shims are not required. The adjustable mounting plates are positioned such that there is contact between the tabs of the rear strut and the mounting plates

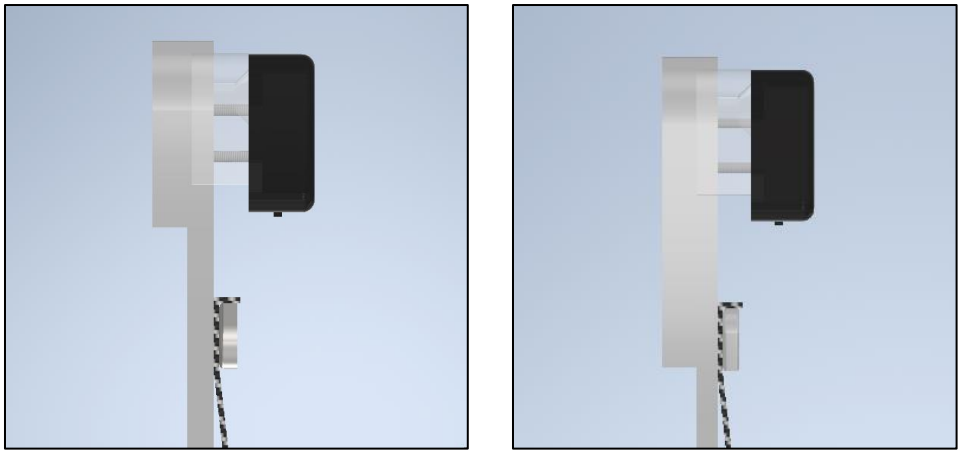

Fig. 23. Modification to the original design of the strut support – extension of the spacer. The upper end of the Al strut is shown for the original design (left) and the revised design (right). The spacer on the left side was lengthened to extend down under the connection to the carbon fiber strut.

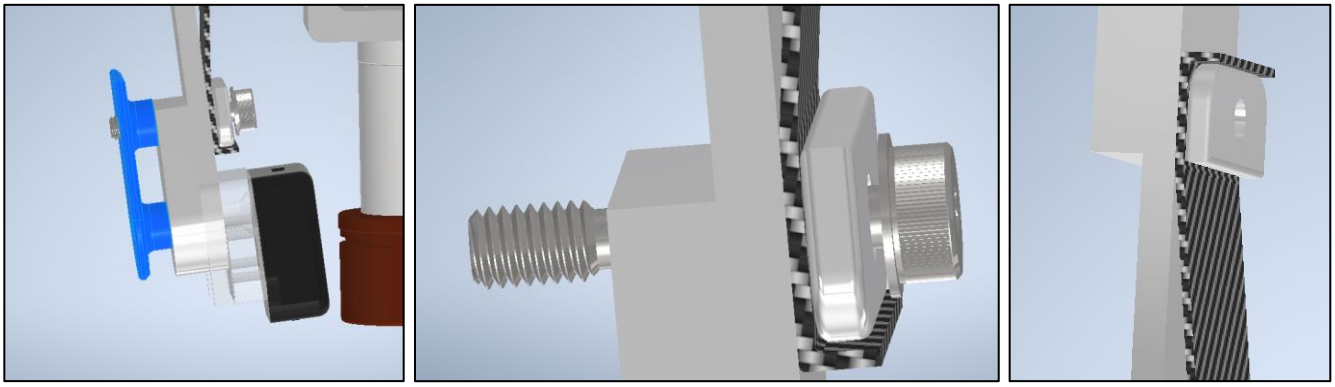

Fig. 24. Change to the carbon fiber strut attachment. Modification to the bottom end of the struts is shown. A shoulder bolt goes all the way through the Al strut, carbon fiber strut, and restraint plate. The black box is the bottom IMU sensor (discussed below).

Strut stiffness test results are included in the *AFT Testing* section below.

Addition of motor-driven angular adjustment

Because we may need to adjust ankle angle when strut stiffness adjustments are made, we created a motor-driven angular adjustment system (Fig. 25). An adjustable ankle mount component is inserted in between the footplate and the Al strut. The ankle mount is attached to a strut mounting bracket using an ankle shaft. The ankle shaft allows the ankle mount and the strut mounting bracket to rotate independent of each other.

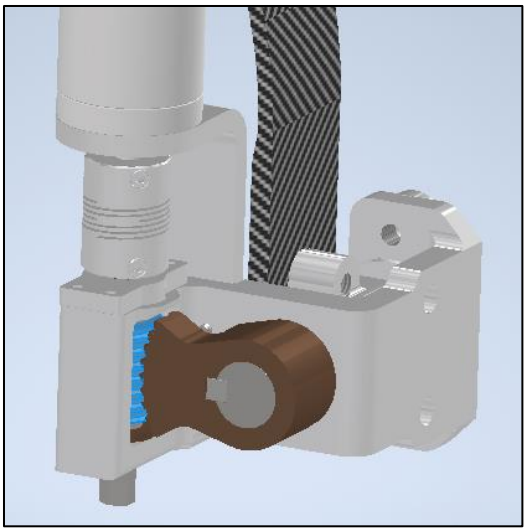

Fig. 25. Motor-driven DAFO angle adjustment mechanism.

The angle of these two components is constrained by a motor that actuates a worm gear / worm wheel system to rotate the ankle mount and control the angle of the footplate. An initial design (Fig. 26, left) had a lot of play in the bearings and the shafts. In addition, the main shaft was not strong enough to hold up to the applied force during running. The new version (Fig. 26, right) uses bushings, tighter tolerances, and bigger shafts to solve the issues. The angle adjustment range is 20 degrees in either direction.

It is recognized that the strut is physically located further away from the back of the leg compared with the mechanism that adjusts strut stiffness (Fig. 19b). We expect that once we have acquired preliminary data using the design and characterized system performance needs, the mechanism will be redesigned accordingly.

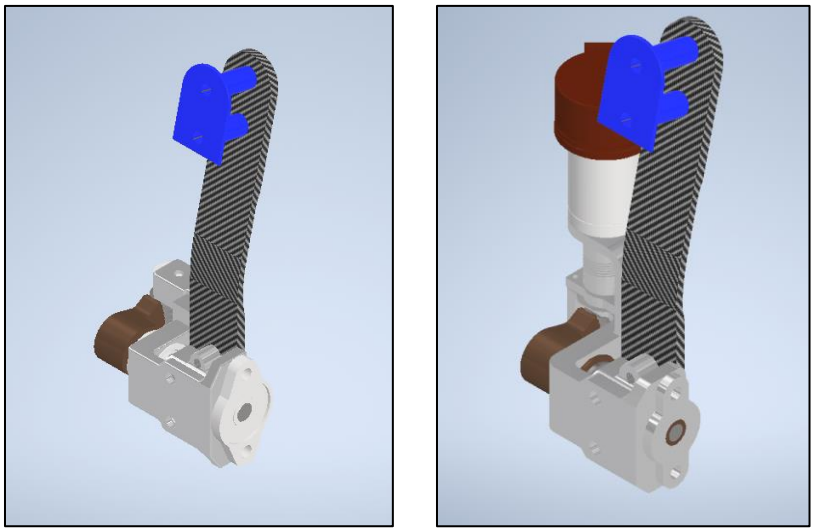

Fig. 26. Design modifications. The initial design (left) had too much play in the bearings and shifts. The revised design (right) uses bushings, tighter tolerances, and bigger shafts, overcoming the problem.

Sensor and Electronic Updates

IMU Ankle Angle Measurement

Results from participant testing demonstrated that the footplate bending strain data was not consistent with the interpretation that it accurately recorded the DAFO deflection. We had anticipated this result in the grant application and proposed to add additional strain gages to monitor axial force in the footplate simultaneously and then combine that data with the bending strain data to calculate the angle. However, for participants with a thin foot, the footplate strain gage axial force measurement had a lot of error. This may have been due to the lack of a uniform footplate thickness in the region of strain gage location in the DAFO. We therefore changed to direct angle measurement of DAFO deflection. Two 9-axis IMUs, one attached to the cuff and one to the footplate, are used (Fig. 27). The difference between the incline angle measured by the two IMUs is used to determine the DAFO deflection. A 3D-printed part was designed to connect the IMUs to the strut.

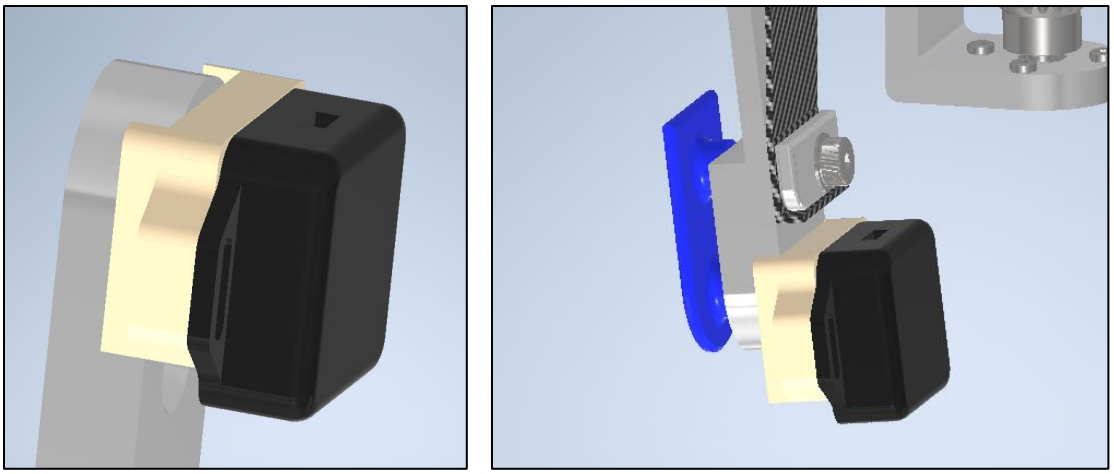

Fig. 27. Mounting the IMUs. IMUs, shown in black, are mounted at (a) the upper end and (b) the lower end of the Al strut using custom designed 3D printed part (yellow).

In our initial design, the IMUs sent data to a LabVIEW VI on an offboard computer. This method required that accelerometer data be aligned with strain gage data in post processing since strain gage data were collected using a different system, a custom on board data logger, termed the ECHO. With the integration of a LattePanda data collection board mounted to the cuff of the DAFO, we were able to run an updated LabVIEW VI and eliminate the need for a benchtop laptop data collection system. Furthermore, by replacing the IMUs with a different product for serial communication (I^2C) with remote data collection devices (WIT901B), we were able to incorporate all data acquisition directly into the ECHO. All data are sampled at 200 Hz. Participant testing demonstrated that the power switches from the IMUs needed to be removed since we were getting triggers from contact with the side of the enclosure during high impact steps. The IMUs now record high quality data.

Footplate Strain Gages

While the glue to affix the strain gages to the footplate cures, it is essential that force be applied evenly over the surface. Several strain gages needed to be replaced in our initial instrumented footplates because this criterion was not accomplished. To overcome the problems, we fabricated custom molds for each footplate from epoxy putty (Smooth-On Free Form AIR HT) conformed to the surface. Two molds were required, one for the top and the other for the bottom (Fig. 28).

Fig. 28. Revised clamping procedure for holding the strain gages to the footplate during curing. Custom molds are fabricated, and a spring clamp is used.

Flexible printed circuit boards (PCBs) were designed to replace many of the connection wires within the strain gage Wheatstone bridge circuits (Fig. 29). The flexible PCB is adhered to the footplate using a flexible silicone epoxy to reduce vibration and mitigate the risk of wire failure during running.

To fabricate the molds, the Free Form material is placed on the surface of the footplate. Cellophane wrap is applied between the putty and the surface to keep the materials from bonding during the cure. A metal plate is applied to the top of the putty to provide a flat clamping surface. The footplate is fit into a vice and left to cure overnight. This procedure ensures that the flat clamping surface for the internal and external molds are parallel to each other. This improved clamping method allows us to bond all 4 strain gages on each side of the footplate at the same time, reducing the number of strain gage cures to 2, thereby

improving manufacturability.

A uniform thickness silicone rubber pad is placed on top of the strain gages between the mold and footplate, and a C clamp fastened in place. The C clamp is spring-loaded to ensure a consistent force is applied despite thermal expansion changes introduced by curing in a high temperature oven.

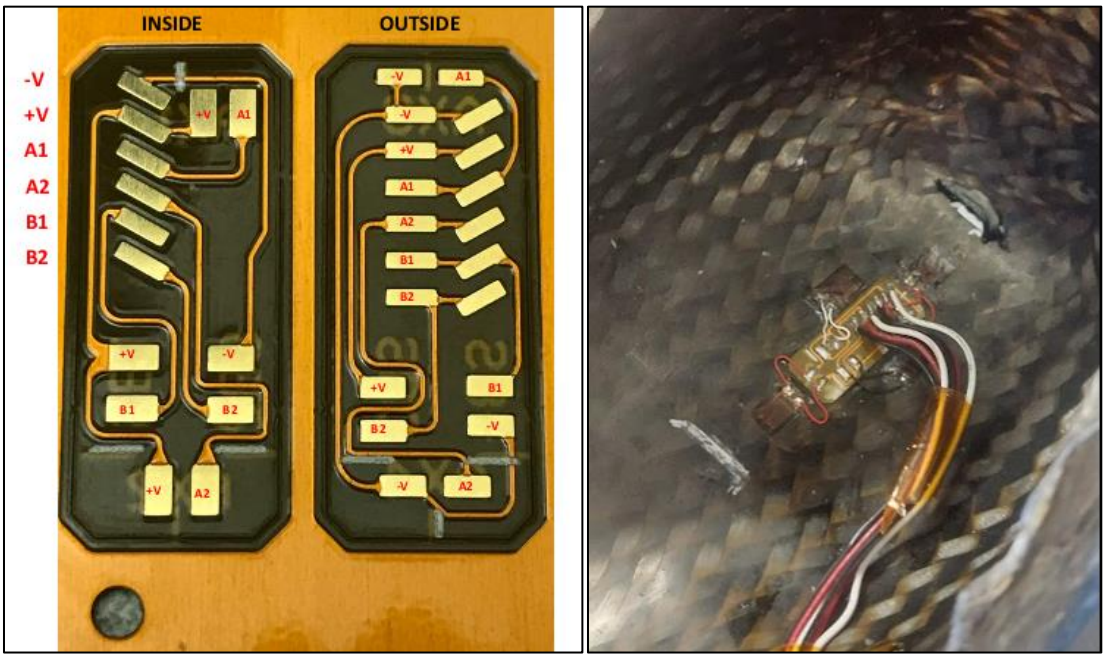

Fig. 29. Flex PCB circuits used to replace wires in the Wheatstone bridge circuit for the strain gages. One flex PCB is placed on each side of the footplate (left). The number of necessary wires is reduced (right).

The flex PCB is covered with a custom-made enclosure designed to match the curvature of the footplate surface (Fig 30). The shape of the footplate is measured using a high-resolution coordinate measurement machine, the part designed using computer-aided design software and then 3D printed. During walking and running, the enclosure protects the strain gages from impact with the participant's heel on the interior surface and the shoe on the exterior surface. A foam insert with a section cut out for the cover is affixed to the inside surface of the footplate.

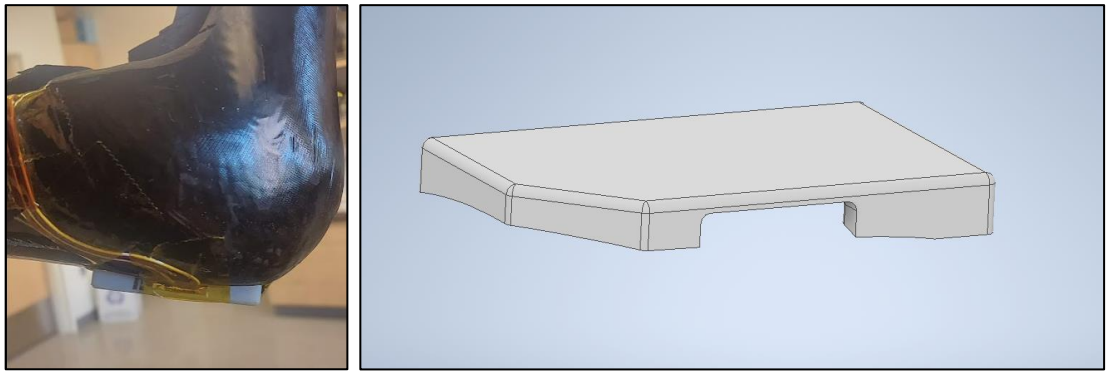

Fig. 30. Cover for strain gages. A cover custom shaped to the individual instrumented footplate is used.

ECHO Data Acquisition System Revision

The ECHO data acquisition system, originally designed by our group for use in prosthetics research, was modified for use in this orthotics application. Two additional general purpose ADC channels were added. The ECHO collects data from both the axial and bending strain gage channels as well as the IMUs. The board is mounted on the cuff of the DAFO so must be protected from impact during take-home use (Fig. 31). Wires exiting the ECHO must be properly strain relieved to avoid mechanical failure problems.

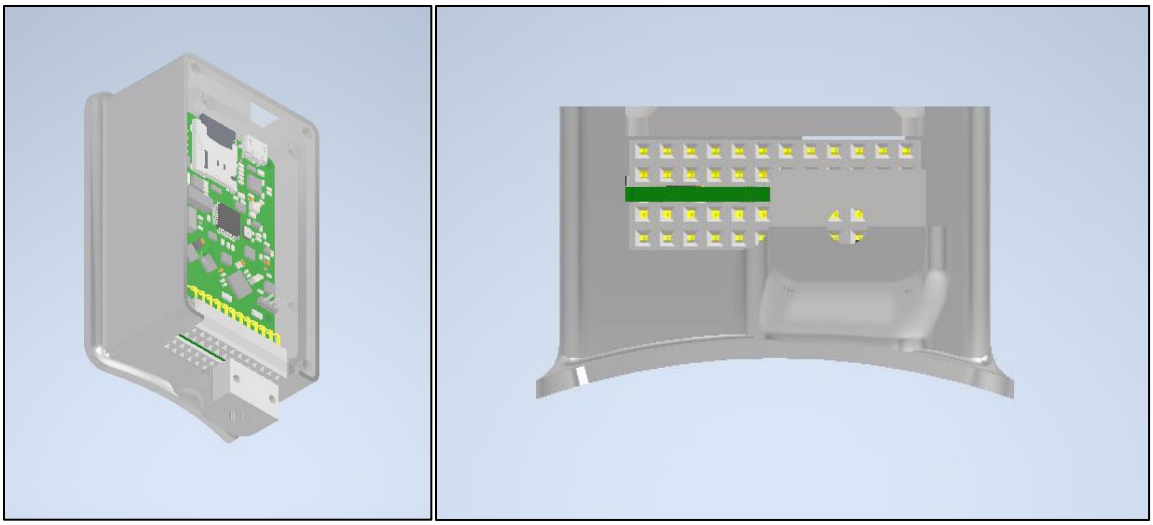

Fig. 31. Instrumentation box to hold the data acquisition system electronics.

The ECHO input/output sensor connector uses a pinned system for flexibility in sensor configuration, allowing it to accommodate a wide range of sensor types. For this project, I^2C connections were required for the IMUs, and general-purpose ADC connections were required for two strain gage channels. The connector itself is not locking and a pulled wire can easily pull the pins from the connector resulting in a loss of signal during a session. As such a clamp was added to the enclosure itself to strain relieve the wires and keep them from coming loose due to vibration or a strained wire. A second modification was to add a curved base for mounting the enclosure so that it fit flush with the surface of the cuff. The cuff was easily bonded to the 3D printed material using epoxy.

The enclosure for the circular strain gage amplifier board that connects the strain gages to the ECHO was modified to mount to the proximal aspect of the footplate lateral surface (Fig. 32). A 3D printed part was designed to include a wire clamp to strain relieve the cable entering the housing.

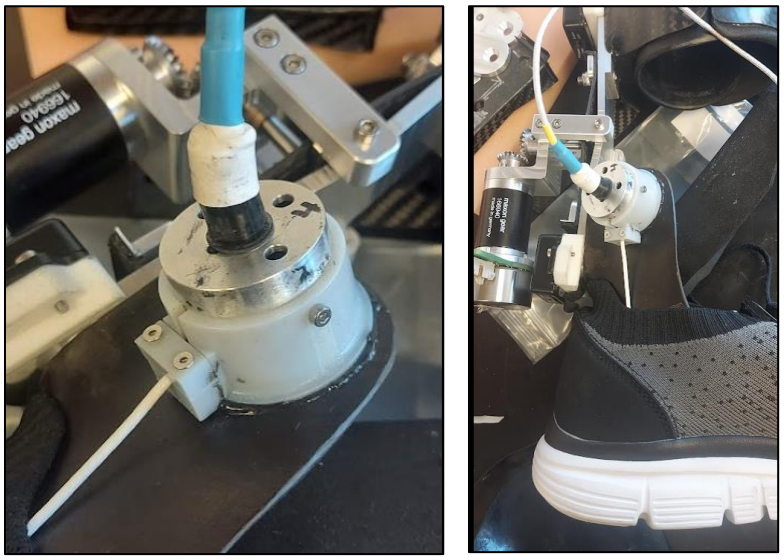

Fig. 32. Updated support assembly for the footplate strain gage signal conditioners. The support housing (white) is affixed to the proximal aspect of the footplate. The wire extending from the signal conditioners to the data acquisition unit on the cuff is strain relieved.

AFT Testing

We observed during our initial able-bodied subjects testing that modifying the strut spacing had little effect on our response variables. Although a notable stiffness response was observed under uniaxial transverse loading in our material testing machine, the loading configuration on the DAFO is much different during clinical use. In an effort to more accurately test the stiffness response of the adjustable strut system, we secured it in a programmable gait simulator that we developed as part of a prior project (Fig. 33). Under a consistent peak stance phase load, the deflection angle of the AFO was measured using the upper and lower IMUs.

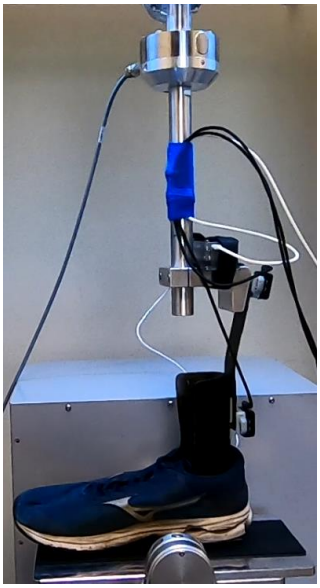

Fig. 33. Ankle foot tester (AFT). This is a gait simulator machine that allows controlled static or cyclic loads to be applied to the DAFO.

Four PDE struts (ratings of 1, 3, 5, and 7) were tested in a randomized order under a load of 200 N to collect a baseline standard for deflection. The adjustable strut assembled with a 4.1 mm Al strut and carbon fiber strut was then tested under the same 200 N loading at the strut spacing conditions of 0 mm, 1 mm, 2 mm, 3 mm, 4 mm, and 5mm presented in a random order. The adjustable strut was additionally tested with the posterior strut removed.

The results confirmed our suspicions that the spacing adjustments made to the posterior strut were not enacting the desired stiffness response. The change in DAFO deflection between the PDE-3 and PDE-5 struts, the range used in our participant testing, was 2.2 degrees, while the change in DAFO deflection between 0 mm and 5 mm strut spacing was only 0.45 degrees (Fig. 34).

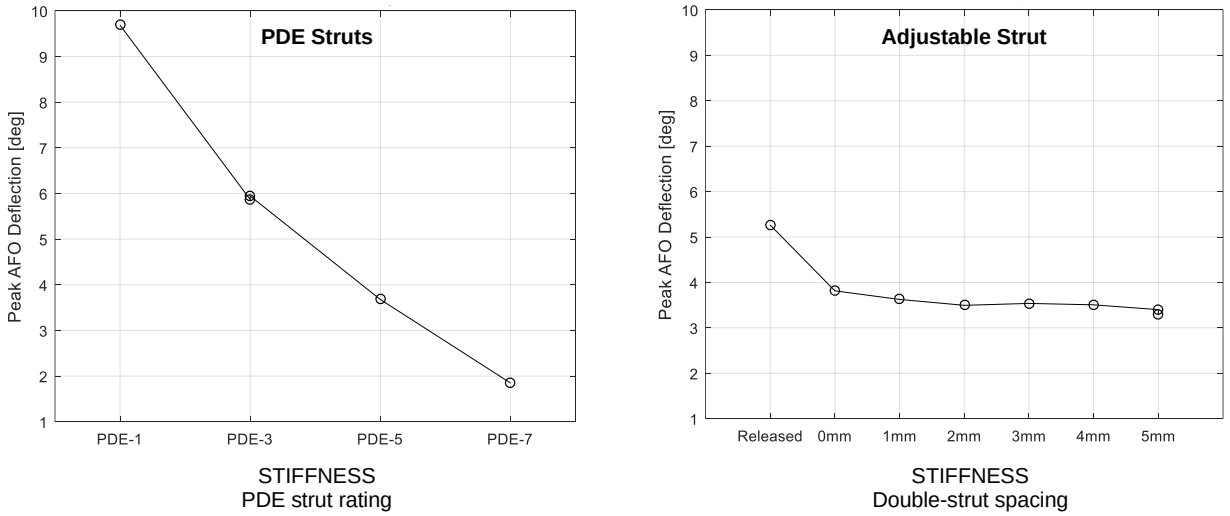

Fig. 34. Deflection angle across the stiffness range. Left: Results from testing a series of PDE struts of different stiffness rating. Right: Results from testing the adjustable strut.

Although deflection decreased approximately linearly with strut spacing across the 0 mm to 5 mm range, the magnitude of the response was approximately 20% of that desired. Upon visual inspection of strut bending, we hypothesized that bending was occurring superior to the span of the carbon fiber strut. To relocate bending to within the carbon fiber region, we extended the spacers located at the ends of the Al strut (Fig. 19b).

To characterize stiffness using the gait simulator data, we defined strut stiffness (k_{strut}) using an applied load of 250 N:

$$k_{strut} = \frac{250\ N}{AFO\ Deflection\ (^o)}$$

A 250 N load was selected since it produced deflections in the PDE struts in the upper half of the range measured on study participants. DAFO deflection was monitored using the difference in angle between the cuff and the footplate, measured by the IMUs. We considered this methodology appropriate because DAFO deflection was approximately linearly related to gait simulator load (Fig. 35). The controller in the gait simulator failed to produce a smooth curve during loading to the first peak thus presence of the nonlinearity in the loading part of the curve in the figure. During simulated running, which is a single peak curve with essentially no heel lever arm, we would expect improved linearity from the start of loading to the peak deflection.

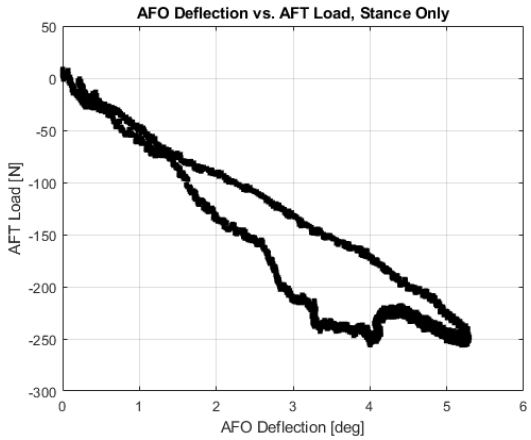

Fig. 35. Results from gait simulator walking. The DAFO deflection is approximately linearly related to the AFT load.

Testing the DAFO with an extended spacer showed improved results over the regular spacer (Fig. 36). Both spacers were 8 mm thick. The spacing testing order was 0, 2, 4, 2, and 0 mm, so that hysteresis could be assessed. Results demonstrated at stiffness increase from 12% for the standard spacer to 35% for the extended spacer. The hysteresis was expected due to slippage between the carbon fiber strut, the Al strut, and the restraint plates used to secure the carbon fiber strut.

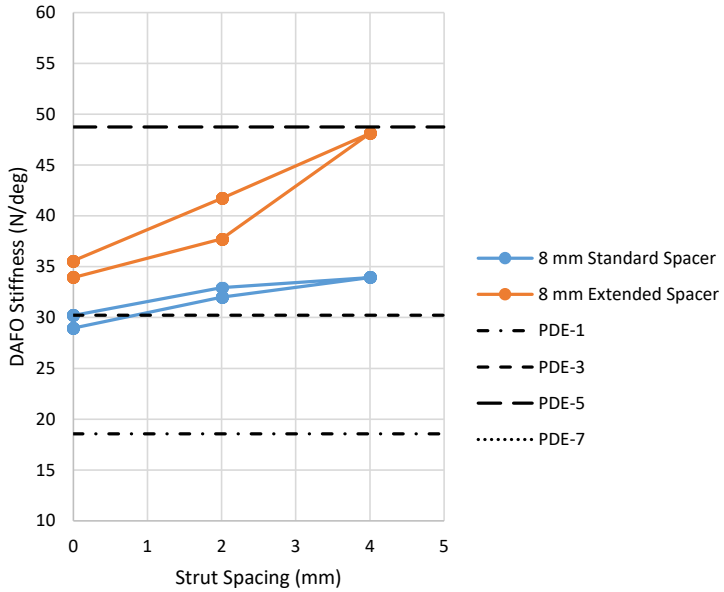

Fig. 36. Comparison of strut stiffness results for an extended spacer compared with the standard spacer. The extended spacer increased the stiffness range of the adjustable strut.

We hypothesized that a loose connection would reduce the variability in slip and thus reduce the hysteresis. We investigated how the torque applied to the bolts holding the restraint plate in place (Fig. 24) affected performance. Three torques were tested: 5, 10, and 12 N·m. Previously, a torque of approximately 10 N·m was used. Results demonstrated a greater stiffness range across the strut spacing range for the 5 N·m torque (58% of the Al strut stiffness) compared with 10 N·m and 12 N·m torques (22% and 16%, respectively) (Fig. 37). Additionally, there was minimal difference in stiffness between the 2 mm and 4 mm strut spacing for the 10 N·m and 12 N·m torques. The difference in response is likely due to the difference in slip of the carbon fiber strut at its anchor points. When too secure, slippage is mitigated, and the system becomes overly stiff with diminished stiffness change from adjustment of the strut spacing. When slip is allowed to occur, a consistent stiffness response is observed that is independent of the previous strut spacing setting. A 5 N·m torque will be used in future studies, and gun oil will be applied to interfaces between the carbon fiber strut, Al strut, and outer restraint plates to facilitate slip.

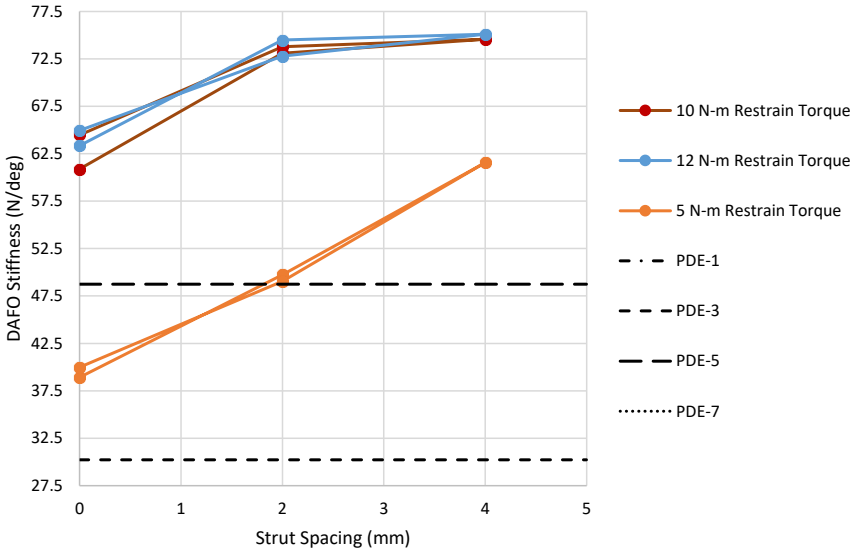

Fig. 37. Effect of restraint torque on the stiffness range of the adjustable strut. A lower torque (5 N·m) increased the stiffness range over a 10 or 12 N·m torque.

The outsourced carbon fiber struts that were fabricated too short (Table 6) demonstrated a stiffness response from the 0 mm to 4 mm strut spacing of only 24%, much less than the 58% above. We hypothesized that because these struts had space between the carbon fiber strut and the restraint plate, they allowed the carbon fiber strut to slip during loading, reducing the stiffness range. When shims were placed between the carbon fiber strut and the restraint plate (Fig. 38), the stiffness range improved from 24% to 40% (Fig. 39).

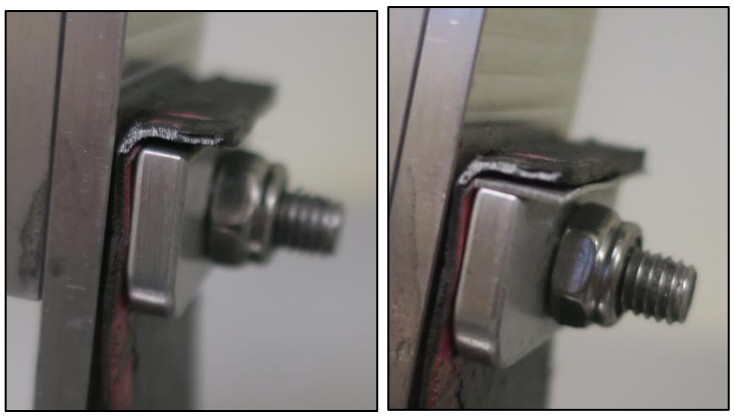

Fig. 38. Shims introduced at the ends of the carbon fiber strut. The shims are placed between the restraint plate and end of the strut.

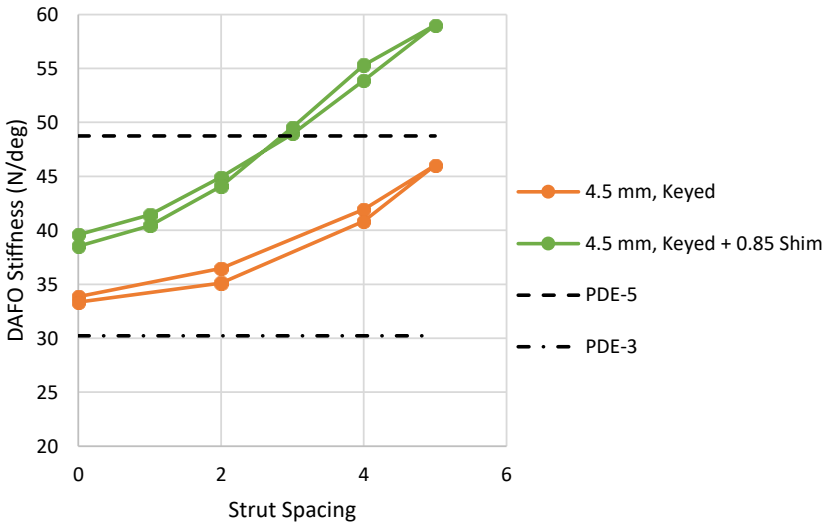

Fig. 39. Effects of adding the shims. The shims increased the range of the adjustable strut stiffness.

To facilitate the design of Al struts for people whose weight, height, and shoe size put them in the lower part of the PDE range (PDE-1 to PDE-3), we tested 4 Al struts ranging in thickness from 4.5 to 6.0 mm with the extended spacers and the shimmed carbon fiber strut in place. Results suggest a 3.75 mm Al strut may be necessary (Fig. 40). We are investigating other material options for the rear strut since this thickness will be difficult to machine.

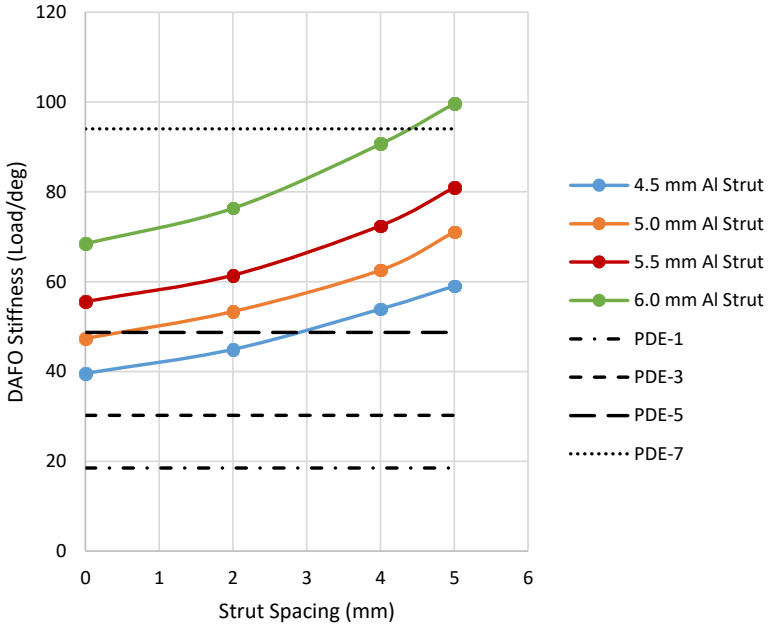

Fig. 40. Stiffness of Al struts of different thickness. These results help to estimate the necessary Al strut thickness for a PDE-1 and PDE-2 strut.

What opportunities for training and professional development has the project provided?

Nothing to Report.

How were the results disseminated to communities of interest?

We failed to report this conference presentation last year:

Weissinger MJ, Allyn KJ, Hughes D, Vamos AC, Carter RV, Wang H, Larsen BG, DeGrasse N, Garbini JL, Friedly JL, Hafner BJ, Sanders JE. An adjustable dynamic AFO operated using a phone app. *American Academy of Orthotists & Prosthetists 47th Academy Annual Meeting & Scientific Symposium*, May 4-7, 2021

What do you plan to do during the next reporting period to accomplish the goals?

Our plan is test at least 3 participants with ankle disability during Year 2 – first the manually-adjusting system and then the auto adjusting system. Data will be prepared for analysis and discussed among the investigators.

4. IMPACT:

What was the impact on the development of the principal discipline(s) of the project?

There is enthusiasm for our strategy of on-board sensing and implementation. Most prior research in this area has been conducted in a gait laboratory – a body of literature that has helped us move this project forward quickly but has limitations towards the objective of an on-board auto adjusting DAFO.

What was the impact on other disciplines?

Nothing to Report.

What was the impact on technology transfer?

Nothing to Report.

What was the impact on society beyond science and technology?

Nothing to Report.

5. CHANGES/PROBLEMS:

Changes in approach and reasons for change

A DAFO plantarflexion/dorsiflexion adjustment was added. IMUs were added to detect DAFO deflection.

Actual or anticipated problems or delays and actions or plans to resolve them

We experienced delays when the company we hired for outsourcing carbon fiber strut fabrication failed to produce a useable strut and then moved away. Our solution was to make the carbon fiber struts in our lab and to investigate other materials so that the struts can be machined.

Changes that had a significant impact on expenditures

Nothing to Report.

6. PRODUCTS:

Nothing to Report.

7. PARTICIPANTS & OTHER COLLABORATING ORGANIZATIONS

What individuals have worked on the project?

Name:	Joan Sanders, PhD
Project Role:	PI
Researcher Identifier (ORCID ID):	0000-0002-8850-243X
Nearest person month worked:	1
Contribution to Project:	Dr. Sanders coordinates the project, communicating regularly with Dr. Garbini and the research engineers on study-related issues

Name:	Joseph Garbini, PhD
Project Role:	Research Engineer
Researcher Identifier (ORCID ID):	
Nearest person month worked:	1
Contribution to Project:	Mechanical design and control system design

Name:	Mathew Weissinger
Project Role:	Research Engineer
Researcher Identifier (ORCID ID):	
Nearest person month worked:	3
Contribution to Project:	Mechanical design

Name:	Ryan Carter
Project Role:	Research Engineer
Researcher Identifier (ORCID ID):	
Nearest person month worked:	2
Contribution to Project:	AFO fabrication

Name:	Katheryn Allyn
Project Role:	Research Prosthetist
Researcher Identifier (ORCID ID):	
Nearest person month worked:	1
Contribution to Project:	Clinical advisor, orthotic support, recruitment

Name:	Bailey Ramesh
Project Role:	Research Engineer
Researcher Identifier (ORCID ID):	
Nearest person month worked:	2
Contribution to Project:	Control system development

Name:	Gabriel Lake
Project Role:	Research Engineer
Researcher Identifier (ORCID ID):	
Nearest person month worked:	1
Contribution to Project:	Electronic design

Name: Adam Krout
Project Role: Research Engineer
Researcher Identifier (ORCID ID):
Nearest person month worked: 3
Contribution to Project: Mechanical design

Name: Kendrick Coburn
Project Role: Research Engineer
Researcher Identifier (ORCID ID):
Nearest person month worked: 3
Contribution to Project: Sensor and instrumentation preparation

Name: Joseph Mertens
Project Role: Research Engineer
Researcher Identifier (ORCID ID):
Nearest person month worked: 3
Contribution to Project: Data collection

Name: Nicholas DeGrasse
Project Role: Research Engineer
Researcher Identifier (ORCID ID):
Nearest person month worked: 3
Contribution to Project: Study execution

Name: Daniel Ballesteros
Project Role: Research Engineer
Researcher Identifier (ORCID ID):
Nearest person month worked: 3
Contribution to Project: Data processing and presentation

Has there been a change in the active other support of the PD/PI(s) or senior/key personnel since the last reporting period?

SANDERS, JOAN E
New grant that has started:
R01HD103815 (Sanders)
National Institutes of Health – National Institute of Child Health and Human Development
"An automatically-adjusting prosthetic socket for people with transtibial amputation"

GARBINI, JOSEPH L
New grant that has started:
R01HD103815 (Sanders)
National Institutes of Health – National Institute of Child Health and Human Development
"An automatically-adjusting prosthetic socket for people with transtibial amputation"

What other organizations were involved as partners?

Nothing to Report.

8. SPECIAL REPORTING REQUIREMENTS

QUAD CHART:

An Automatically Adjusting Dynamic Orthosis to Enhance Performance of Warfighters with Lower Limb Injury

Log Number: DM190651
Award Number: W81XWH2010908
PI: Joan Sanders Ph.D. **Org:** University of Washington **Award Amount:** $1.5M

Study Aims

- **Aim 1:** Create a motor-driven, variable-stiffness dynamic brace that adjusts across a stiffness range of 5 PDE-MCSS levels using a cell phone app
- **Aim 2:** Create a controller algorithm that adjusts strut stiffness for varying running speeds and terrains to maintain users' maximum dorsiflexion and ankle angle range near but not beyond their acceptable limits
- **Aim 3:** Conduct a randomized crossover study to compare performance of the automatic stiffness-adjusting dynamic brace to a traditional brace

Approach

A current prototype is extended into a fully functional design. Treadmill studies are conducted to identify relationships between strut stiffness and ankle angle across a range of running speeds and terrains. An algorithm to automatically adjust strut stiffness based on ankle angle is implemented in an on-board micro-controller. Activity is recorded while participants wear each brace (automatic, traditional) in their free-living environments for 4 weeks, and functional test and self-report data are collected. The automatic brace is expected to enhance running speed, endurance and user satisfaction.

Motor-driven adjustable strut system. A motor at the bottom left drives a gear that adjusts the spacing between an aluminum inner strut and a carbon-fiber outer strut, effecting a change in strut stiffness. Sensors affixed to the footplate monitor the sagittal plane bending, and IMUs fastened to the upper and lower part of the system monitor the cuff-footplate angle. A data acquisition system is fastened to the side of the cuff. The system has been used on able-bodied participants running on the treadmill in the lab and outdoors on a nearby jogging trail.

Timeline and Cost

Activities CY	20	21	22	23
Aim 1: Enhance prototype design				
Aim 2: Conduct lab testing				
Aim 3: Conduct small crossover study				
Estimated Budget ($K)	**$346**	**$383**	**$379**	**$392**

Updated: 10/15/2022

Goals/Milestones
CY20 Goal – Finish design, IRB/HRPO approval, begin recruitment
☒ Optimize geometry, add motor and mobile phone control
☒ Characterize quality of measurement and operation
☒ Accomplish IRB and HRPO approval
☒ Recruit participants for lab testing
CY21 Goals – Continue lab testing, begin crossover study
☒ Assess relationships of ankle angle, strut stiffness, and run speed
☒ Recruit lower-limb injured participants for crossover study
CY22 Goals – Continue crossover study, begin to assess data
☐ Continue 4-week testing in participant free-living environments
☐ Compare data from intervention and control configurations
CY23 Goals – Complete crossover study and outcomes analysis
☐ Disseminate results
☐ Prepare final report
Comments/Challenges/Issues/Concerns
• COVID-19 issues are causing parts and supplies delays
Budget Expenditure to Date $846,006

9. APPENDICES

Appendices Table of Contents

Stiffness-Gait Protocol

GENERAL

Materials

- AFO assembly
- PDE-3 and PDE-5 strut
- 2 WT901BLECL WitMotion IMUs w/ attachment adapters
- Echo board
- Micro SD card
- 2 USB C cables
- Waist belt
- GoPro w/ high frame rate

Other

- Lookup testing order for participant on common disk

Stiffness-Gait Protocol			
START TIME	ACTIVITY	DETAILS	NOTES
	Assemble AFO	Use PDE strut appropriate for user	
	Start Echo	Connect to Echo in HTerm Make sure SD card is recognized Turn on strain channels 1 and 2 Configure sampling frequency to 200 Hz using 'f 200' Test that strain values are as expected ~25,000 counts and sampling frequency is correct.	
	Start Labview VI	Connect to LattePanda using *TightVNC* Double check proper COM port configuration to IMUs Start collection and make sure both data streams are coming in	
	Doffed AFO Zero	Hold AFO upright off of the floor to get a zero reading	
	Don AFO, Check Fit	Start up the treadmill and have the participant use this time to test out the AFO while walking; make any necessary changes to fit, padding, etc. Find preferred walking and jogging speeds and record	Preferred Walking Speed:_____ Preferred Jogging Speed:_____
	Sit	Have the participant move from the treadmill to the participant lab chair	
	Donned Zero	Participant supports with hands just behind knee. Lift AFO off the ground and relax ankle such that no active internal moment is applied	

Protocol 1: Ankle Activation

Perform a 30 second trial under each of the following conditions

Trial #	Gait	Ankle Activity	Completion Time
1	Walk	Active	
2	Walk	Inactive	
3	Jog	Active	
4	Jog	Inactive	

Protocol 2: Speed & Gait

Perform a 30 second jogging trial under each of the following conditions.
Aim to keep an inactive ankle.

Stiffness	Gait	Completion Time	Inactive Ankle? (y/n)
Strut 1:	Gait 1:		
Strut 1:	Gait 2:		
Strut 1:	Gait 3:		
Strut 1:	Gait 4:		
Strut 2:	Gait 5:		
Strut 2:	Gait 6:		
Strut 2:	Gait 7:		
Strut 2:	Gait 8:		

	Synchronization	Gently stomp with the AFO several times	
	End collection	Stop the IMU collection Connect to Echo via HTerm and stop the collection Check that Echo data looks good. Label appropriately. Label IMU data appropriately	

Ankle Angle-Outdoor Terrain Protocol

GENERAL

Materials

- AFO assembly
    - Appropriate PDE strut
    - AFO angle adjustment mechanism
    - 2 WT901BLECL WitMotion IMUs w/ attachment adapters
- Echo board
- Micro SD card
- 2 USB C cables
- Laptop with TightVNC
- LattePanda
- Anker Astro E3 power pack
- Waist belt
- GoPro w/ high frame rate

Other

- One revolution angle adjustment mechanism = 7.2 degrees
- 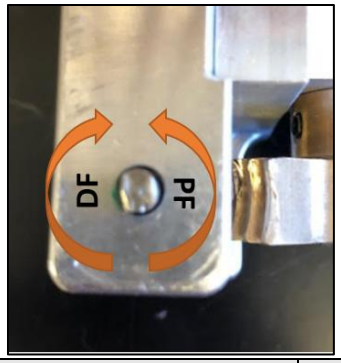

7° Plantarflexion	Neutral	7° Dorsiflexion
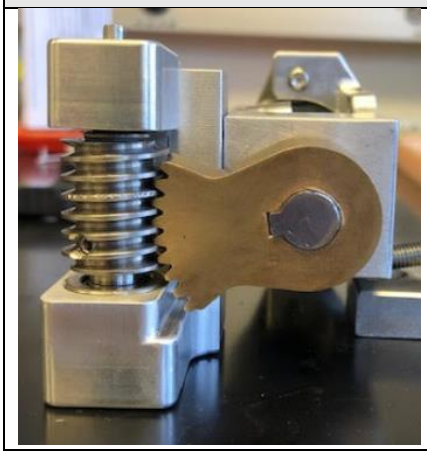	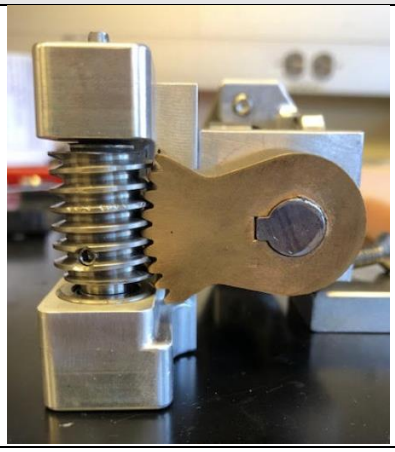	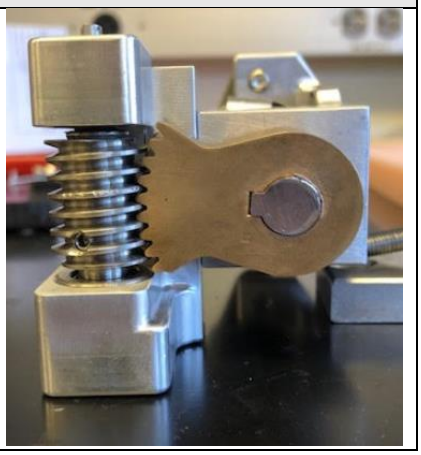

Ankle Angle Outdoor Terrain Protocol

START TIME	ACTIVITY	DETAILS	NOTES
	Go to testing location 1	Proceed to the flat section of the Burke-Gilman Trail across the street	
	Instruct participant	Remind participant to aim to emulate an inactive ankle within the AFO	
	Start Echo	Connect to Echo in HTerm Make sure SD card is recognized Turn on strain channels 1 and 2 Configure sampling frequency to 200 Hz using 'f 200' Test that strain values are as expected ~25,000 counts and sampling frequency is correct.	
	Start Labview VI	Connect to LattePanda using TightVNC Double check proper COM port configuration to IMUs Start collection and make sure both data streams are coming in	
	Doffed AFO Zero	Hold AFO upright off of the floor to get a zero reading	
	Don AFO	Take this time to test out the AFO while walking and make any necessary changes to fit, padding, etc. Walk down the trail for 30 seconds, then return. Jog down the trail for 30 seconds then return. This will establish the end points for the following tests.	
	Sit		
	Adjust AFO Angle	Set AFO angle to Condition 1 for this participant	AFO Angle 1:_____
	Donned Zero	Support with hands just behind knee. Lift AFO off the ground and relax ankle such that no active internal moment is applied	

	Walk	Walk for 30 seconds down a flat section of the trail	
	Stand	Stand for ~5 seconds	
	Walk	Return back to the starting point	
	Stand	Stand for ~5 seconds	
	Jog	Walk for 30 seconds down a flat section of the trail	
	Stand	Stand for ~5 seconds	
	Jog	Return back to the starting point	
	Adjust AFO Angle	Set AFO angle to Condition 2 for this participant	AFO Angle 2:_____
	Donned Zero	Support with hands just behind knee. Lift AFO off the ground and relax ankle such that no active internal moment is applied	
	Walk	Walk for 30 seconds down a flat section of the trail	
	Stand	Stand for ~5 seconds	
	Walk	Return back to the starting point	
	Stand	Stand for ~5 seconds	
	Jog	Walk for 30 seconds down a flat section of the trail	
	Stand	Stand for ~5 seconds	
	Jog	Return back to the starting point	
	Adjust AFO Angle	Set AFO angle to Condition 3 for this participant	AFO Angle 3:_____
	Donned Zero	Support with hands just behind knee. Lift AFO off the ground and relax ankle such that no active internal moment is applied	
	Walk	Walk for 30 seconds down a flat section of the trail	
	Stand	Stand for ~5 seconds	
	Walk	Return back to the starting point	
	Stand	Stand for ~5 seconds	
	Jog	Walk for 30 seconds down a flat section of the trail	
	Stand	Stand for ~5 seconds	
	Jog	Return back to the starting point	

	Stand	Stand for ~5 seconds	
	Synchronization	Gently stomp with the AFO several times	
	Check Data	Stop Echo collection, process data and check that everything looks as expected. Label files appropriately Stop IMU collection. Label files appropriately Restart Echo and IMU collections Set AFO to neutral position	
End of Flat Trials | Start of Hill Trials			
	Go to testing location 2	Proceed to the hill near the George Washington statue	
	Instruct participant	Remind participant to aim to emulate an inactive ankle within the AFO	
	Adjust AFO Angle	Set AFO angle to Condition 1 for this participant	AFO Angle 1:_____
	Walk	Walk up hill	
	Stand	Stand for ~5 seconds	
	Walk	Walk down hill	
	Stand	Stand for ~5 seconds	
	Walk	Walk up hill	
	Stand	Stand for ~5 seconds	
	Walk	Walk down hill	
	Stand	Stand for ~5 seconds	
	Jog	Jog up hill	
	Stand	Stand for ~5 seconds	
	Jog	Jog down hill	
	Stand	Stand for ~5 seconds	
	Jog	Jog up hill	
	Stand	Stand for ~5 seconds	
	Jog	Jog down hill	
	Stand	Stand for ~5 seconds	
	Adjust AFO Angle	Set AFO angle to Condition 2 for this participant	AFO Angle 2:_____

	Walk	Walk up hill	
	Stand	Stand for ~5 seconds	
	Walk	Walk down hill	
	Stand	Stand for ~5 seconds	
	Walk	Walk up hill	
	Stand	Stand for ~5 seconds	
	Walk	Walk down hill	
	Stand	Stand for ~5 seconds	
	Jog	Jog up hill	
	Stand	Stand for ~5 seconds	
	Jog	Jog down hill	
	Stand	Stand for ~5 seconds	
	Jog	Jog up hill	
	Stand	Stand for ~5 seconds	
	Jog	Jog down hill	
	Stand	Stand for ~5 seconds	
	Adjust AFO Angle	Set AFO angle to Condition 3 for this participant	AFO Angle 3:_____
	Walk	Walk up hill	
	Stand	Stand for ~5 seconds	
	Walk	Walk down hill	
	Stand	Stand for ~5 seconds	
	Walk	Walk up hill	
	Stand	Stand for ~5 seconds	
	Walk	Walk down hill	
	Stand	Stand for ~5 seconds	
	Jog	Jog up hill	
	Stand	Stand for ~5 seconds	
	Jog	Jog down hill	
	Stand	Stand for ~5 seconds	
	Jog	Jog up hill	
	Stand	Stand for ~5 seconds	
	Jog	Jog down hill	
	Stand	Stand for ~5 seconds	

	Synchronization	Gently stomp with the AFO several times	
	Return to lab		
	End collection	Connect to LattePanda via TightVNC and stop the IMU collection Connect to Echo via HTerm and stop the collection Check that Echo data looks good. Label appropriately. Label IMU data appropriately	

Plant Gain-Treadmill Terrain Protocol

GENERAL

Participant Code:_____ Date: _____

Materials

- Auto-adjusting AFO assembly
- 2 WT901BLECL WitMotion IMUs w/ attachment adapters
- Echo board
- Micro SD card
- 4 USB C cables
- 24 V Power Supply
- Maxon motor controller
- Maxon cable assembly
- Waist belt
- GoPro w/ high frame rate

Configuration

C Strut version		**Echo board version**	
Al Strut thickness		**Echo firmware**	
Shoulder bolt length		**WIT IMU model**	
Should bolt shims			
Al Strut spacers			

Plant Gain-Treadmill Terrain Protocol

START TIME	ACTIVITY	DETAILS	NOTES
	Assemble AFO	Use appropriate Al strut thickness and strut spacer for user	
	Start Labview VIs	Start Read IMU (direct write).vi with IMUs configured appropriately Make sure SD card is recognized by Echo Start Treadmill_V0.vi in TreadMill_AFO_Maxon_NoIMU.llb Make sure Swing Move is enabled and encoder is set to zero.	
	Doffed AFO Zero	Hold AFO upright off of the floor to get a zero reading	
	Don AFO, Check Fit	Start up the treadmill and take this time to test out the AFO while walking and make any necessary changes to fit, padding, etc. Find preferred jogging speed and record	Preferred Jogging Speed:_____
	Sit		
	Donned Zero	Support with hands just behind knee. Lift AFO off the ground and relax ankle such that no active internal moment is applied	
	Flat Plant Gain	Start jogging at preferred speed at 0 mm spacing. Start plant gain and step up to 5 mm. Wait 10 seconds, then begin ramping down strut spacing. Once at 0 mm, wait another 10 seconds.	
	Rest		
	Incline Plant Gain	Set treadmill to 10% grade. Start jogging at preferred speed at 0 mm spacing. Start plant gain and step up to 5 mm. Wait 10 seconds, then begin ramping down strut spacing. Once at 0 mm, wait another 10 seconds.	

	Synchronization	Gently stomp with the AFO several times	
	End collection	End both the IMU collection VI and the Treadmill VI	

Appendix 2: Parts list for stiffness adjustment

No.	Qty	Part	Description
1	1	DAFO-V3-0222	5.0 KEYED STRUT
2	1	DAFO-V3-0006	ANKLE SPACER PLATE, 8 MM
3	1	DAFO-V3-0013	Rear Peace V4
4	2	DAFO-V3-0015	ACCELEROMETER MOUNT
5	1	DAFO-V3-0016	CALF SPACER PLATE 8 MM
6	1	DAFO-V3-0035	SINGLE JACK BAR V3
7	1	DAFO-V3-0103	BOTTOM PLATE
8	1	DAFO-V3-0104	TOP PLATE
9	1	DAFO-V3-0108	MOTOR MOUNT
10	2	DAFO-V3-0109	MOUNTING BAR
11	1	DAFO-V3-0207	STRUT SHAFT
12	1	DAFO-V3-0800	MAXON Motor Assembly
13	2	DAFO-V3-0801	WIT WT901BLECL 5.0 ACCELEROMETER
14	1	DAFO-V3-0802	OIL EMBEDDED FLANGED SLEEVE BEARING, 6 MM ID, 9 MM OD, 10 MM FLANGE
15	2	DAFO-V3-0803	METAL MITER GEAR, MCMASTER 3560N13
16	1	DAFO-V3-0804	FLANGED BALL BEARING, 6 MM ID, MCMASTER 57155K472
17	2	DAFO-V3-0805	AFO ADAPTOR, FABTECH
18	1	DAFO-V3-0806	SHIMS, 6 MM ID, VARIOUS AS NEEDED
19	1	DAFO-V3-0807	SHOULDER SCREW, M6, 6 MM OD SHOULDER, 18 MM LG

Parts list for angle adjustment – in appendix

No.	Qty	Part	Description
1	1	ADJPLTR-V1-0008	WORM GEAR
2	1	ADJPLTR-V1-0011	BUSHING HOUSING
3	1	ADJPLTR-V1-0051	MOUNTING BRACKET
4	1	ADJPLTR-V1-0052	ANKLES SHAFT
5	1	ADJPLTR-V1-0053	GEAR SHAFT
6	1	ADJPLTR-V1-0054	WORM WHEEL
7	1	ADJPLTR-V1-0055	ANKLE MOUNT
8	1	ADJPLTR-V1-0057	CALF MOUNT
9	1	ADJPLTR-V1-0059	UPPER BEARING HOUSING
10	1	ADJPLTR-V1-0066	MOTOR MOUNT
11	1	ADJPLTR-V1-0700	OIL EMBEDDED FLANGED SLEEVE BEARING, 8 MM ID, 12 MM OD, 16 MM FLANGE, 8 MM LG
12	1	ADJPLTR-V1-0701	OIL EMBEDDED FLANGED SLEEVE BEARING, 4 MM ID, 8 MM OD, 12 MM FLANGE, 8 MM LG
13	1	ADJPLTR-V1-0702	EXTERNAL RETAING RING FOR 6 MM OD SHAFT
14	1	ADJPLTR-V1-0703	PRECISION FLEXIBLE SHAFT COUPLING, 6 MM X 4 MM
15	1	ADJPLTR-V1-0704	OIL EMBEDDED FLANGED SLEEVE BEARING, 20 MM ID, 24 MM OD, 28 MM FLANGE, 12 MM LG
16	1	ADJPLTR-V1-0705	OIL EMBEDDED FLANGED SLEEVE BEARING, 8 MM ID, 12 MM OD, 16 MM FLANGE, 12 MM LG
17	1	ADJPLTR-V1-0706	MACHINE KEY, 5 MM X 5 MM X 16 MM
18	1	ADJPLTR-V1-0707	MACHINE KEY, 5 MM X 5 MM X 30 MM

19	1	ADJPLTR-V1-0800	SHIMS, VARIOUS SIZES
20	1	FABTECH STRUT	VARIOUS AVAILABLE
21	1	MAXON Motor Assembly	MAXON MOTOR ASSEMBLY